nature medicine

Article

https://doi.org/10.1038/s41591-022-02060-2

Safety, immunogenicity and effect on viral rebound of HTI vaccines in early treated HIV-1 infection: a randomized, placebo-controlled phase 1 trial

Received: 3 November 2021

Accepted: 28 September 2022

Published online: 27 October 2022

Check for updates

A list of authors and their affiliations appears at the end of the paper

HIVACAT T-cell immunogen (HTI) is a novel human immunodeficiency virus (HIV) vaccine immunogen designed to elicit cellular immune responses to HIV targets associated with viral control in humans. The AELIX-002 trial was a randomized, placebo-controlled trial to evaluate as a primary objective the safety of a combination of DNA.HTI (D), MVA.HTI (M) and ChAdOx1. HTI (C) vaccines in 45 early-antiretroviral (ART)-treated individuals (44 men, 1 woman; NCT03204617). Secondary objectives included T-cell immunogenicity, the effect on viral rebound and the safety of an antiretroviral treatment interruption (ATI). Adverse events were mostly mild and transient. No related serious adverse events were observed. We show here that HTI vaccines were able to induce strong, polyfunctional and broad CD4 and CD8 T-cell responses. All participants experienced detectable viral rebound during ATI, and resumed ART when plasma HIV-1 viral load reached either >100,000 copies ml^{-1}, >10,000 copies ml^{-1} for eight consecutive weeks, or after 24 weeks of ATI. In post-hoc analyses, HTI vaccines were associated with a prolonged time off ART in vaccinees without beneficial HLA (human leukocyte antigen) class I alleles. Plasma viral load at the end of ATI and time off ART positively correlated with vaccine-induced HTI-specific T-cell responses at ART cessation. Despite limited efficacy of the vaccines in preventing viral rebound, their ability to elicit robust T-cell responses towards HTI may be beneficial in combination cure strategies, which are currently being tested in clinical trials.

Therapeutic vaccines designed to enhance human immunodeficiency virus (HIV)-specific T-cell immunity have been postulated to be a key component of any HIV cure strategy[1]. Different therapeutic vaccine candidates have been shown to be safe, immunogenic and able to induce broad and functional T- and B-cell immune responses[2–5]. However, no reduction in HIV-1 viral reservoirs, prevention of viral rebound or suppressed viremia off ART have been reported in randomized, placebo-controlled trials of vaccines, given alone or in combination with latency-reversing agents[5–7].

One potential reason for these suboptimal trial outcomes may have been T-cell immunogen designs and the induction of virus-specific T-cell responses with ineffective or insufficient antiviral activity. To overcome this, HTI (HIVACAT T-cell immunogen)-based vaccines were designed to induce functional HIV-1-specific T-cell responses that were

e-mail: jmolto@lluita.org

associated with better viral control in more than 1,000 HIV-1 clade B and C infected individuals within a broad HLA (human leukocyte antigen) class I and class II allele coverage[8] targeting the most vulnerable sites of HIV-1. The HTI immunogen includes 16 HIV-1 regions from Gag, Pol, Nef and Vif that induce T-cell responses of high functional avidity and cross-reactivity and target regions of overall low diversity/entropy, even though these regions were not predicted by stringent conservation algorithms, but were based on human trial data[9,10]. Importantly, in independent cohorts of viremic controllers and individuals with breakthrough infection after being vaccinated with full-length proteins, recognition of viral protein segments covered by HTI were found to be generally subdominant, but, when detected, were associated with better viral control and viral inhibition of clade-matched HIV isolates[11]. The 16 identified HIV-1 regions were assembled in a 529aa immunogen sequence (HTI) and expressed both in a plasmid DNA (DNA.HTI, D)[12] and two viral-vectored vaccines based on a modified Vaccinia virus Ankara (MVA.HTI, M)[13] and a chimpanzee adenovirus (ChAdOx1.HTI, C)[14].

AELIX-002 was a phase I, first-in-human, randomized, double-blind, placebo-controlled study to evaluate the safety, immunogenicity and effect on viral rebound of DNA.HTI, MVA.HTI and ChAdOx1.HTI HIV-1 vaccines administered in a heterologous prime-boost regimen to 45 virally suppressed, early-treated individuals with HIV-1 infection.

Results

A total of 45 participants (44 men and 1 woman), virologically suppressed for at least one year, were recruited from an existing Early-ART cohort[15]. Acute/recent infection at ART initiation was confirmed based on any of the following criteria: (1) positive plasma HIV-1 RNA with negative serology, (2) positive Gag p24 antigen; (3) indeterminate western blot; (4) absence of the p31 band in a positive western blot in the context of a known exposure/reported acute retroviral syndrome; and/or (5) negative HIV antibody test <24 weeks from the first positive test and before starting ART. Participants were randomized 2:1 to receive vaccines or placebo. DNA.HTI or placebo were given at weeks 0, 4 and 8 and MVA.HTI or placebo were given at weeks 12 and 20. All participants completed the first vaccination regimen (DDDMM (n = 30) or placebo (n = 15)). Of them, 42 reconsented to start a second vaccination regimen after a favorable report from the safety monitoring committee (SMC) once the last participant had reached week 32 of the follow-up. The second vaccination regimen started after a minimum of 24 weeks from last MVA.HTI or placebo vaccination. Participants received ChadOx.HTI or placebo at weeks 0, 12 and MVA. HTI or placebo at week 24. Finally, 41 participants (CCM (n = 26) or placebo (n = 15)) entered an analytical treatment interruption (ATI) eight weeks after completing the last series of vaccination (CCM or placebo; Fig. 1).

Demographics

Table 1 presents the baseline characteristics. ART was initiated after a median (range) of 55 (12–125) and 64 (6–140) days after the estimated date of HIV-1 acquisition in placebo and vaccine recipients, respectively. All participants were receiving an integrase strand transfer inhibitor (INSTI)-based ART regimen at inclusion. Median (range) time with undetectable viral load at enrollment was 18 (13–56) and 27 (12–55) months, and median $CD4^+$ T-cell counts (range) were 826 (549–2,156) and 727 (553–1,336) cells per mm^3 in the placebo and in the vaccine group, respectively (not significant for all parameters). Three placebo (20%) and seven (23%) vaccine recipients expressed any HLA class I allele associated with spontaneous control of HIV replication, respectively (that is HLA-B*27:05, -B*57:01, -B*15:17 and/or -B*15:03). In addition, six (40%) placebo recipients and nine (30%) vaccinees expressed HLA class I alleles associated with HIV disease progression (that is, HLA-B*07:02, -B*08:01, -B*35:01/02/03, -B*53:01 and/or -B*54/55/56)[16].

Pre-ART HIV-1 viral sequencing

Full-genome deep sequencing was performed on HIV-1 viral sequences isolated within the first four weeks of ART initiation from 41 participants. Of the 41 participants, 32 (78%) had subtype B viruses. Phylogenetic distance to a reference sequence (HXB2) and the coverage by the HTI immunogen were comparable between placebo and vaccine recipients for any of the HIV-1 proteins included in the HTI immunogen (Extended Data Fig. 1a–c). The median (range) number of pre-ART CTL (cytotoxic T lymphocyte) escape mutants within sequences included in the HTI immunogen was 7 (2–11) and 5 (2–8) in the placebo and vaccine recipients, respectively (Mann–Whitney, P = 0.0364; Extended Data Fig. 1d). The degree of pre-ART CTL escape in HTI-covered regions was not associated with replication fitness of the participants' autologous virus (Extended Data Fig. 1e).

Safety

The severity and intensity of adverse events (AEs) were assessed by the investigator according to the Division of DAIDS table for grading the severity of adult and pediatric adverse events, version 2.1 (March 2017). Overall, vaccines were safe and well-tolerated (Extended Data Table 1). All participants reported solicited AEs related to vaccinations, which were mostly mild (grade 1–2) and transient, except one participant who reported grade 3 asthenia lasting <72 h after the third MVA.HTI vaccination. A total of 440 related AEs were recorded during the entire vaccination phase (111 in placebo and 329 in vaccine recipients), of which 76 and 229 occurred after placebo or DDDMM administrations and 35 and 100 after placebo or CCM (Supplementary Tables 1–4). The most frequent AEs related to vaccinations were pain at the injection site and a flu-like syndrome. There were only two serious adverse events (SAEs) during the study—an episode of acute infectious gastroenteritis due to *Campylobacter jejuni* and an acute appendicitis that required hospitalization, both in vaccine recipients (Extended Data Table 2). No laboratory abnormalities related to vaccinations were reported.

Immunogenicity

Total HIV-1 and HTI-specific T cells were assessed by an ex vivo interferon (IFN)-γ-detecting enzyme-linked immunosorbent spot (ELISpot) assay. Both vaccination regimens (DDDMM and CCM) were immunogenic. The median (range) increase in the total frequencies of HTI-specific T cells from baseline to the peak immunogenicity timepoint after the overall vaccination regimen was 100 (0–498) spot-forming cells (SFCs) per million peripheral blood mononuclear cells (PBMCs) in the placebo group and 1,499 (120–3,150) in the vaccine group (Mann–Whitney t-test, P < 0.0001; Fig. 2a and Extended Data Table 3). This corresponded to an increase in HTI magnitude of more than twofold in ten (67%) and more than threefold in one (7%) of the placebo recipients compared to 29 (97%) and 24 (80%) of vaccine recipients (Fisher's exact test, P = 0.0117 and P < 0.0001, respectively; Extended Data Table 3). To determine the breadth of vaccine-induced T-cell responses, PBMCs obtained at study entry and after DDDMM and CCM or placebo were expanded in vitro and tested against individual 15-mer overlapping peptides (OLPs) covering the HTI immunogen (n = 147). A cumulative breadth over the entire vaccination period of a median (range) of 5 (1–13) IFN-γ-producing responses to individual HTI-covered OLPs was detected in vaccinees without any specific pattern of immunodominance across the HIV subproteins covered by the HTI immunogen, in contrast to 3 (1–8) and predominantly gag-specific responses in placebo recipients (Mann–Whitney t-test, P = 0.0125; Fig. 2b,c). Responses to HTI were already present in 31 participants (20 vaccine and 11 placebo recipients) before ART was initiated. The maximal magnitude of HTI-specific responses achieved during the intervention phase positively correlated with the magnitude of pre-ART HTI-specific T-cell responses (Spearman's ρ = 0.5343, P = 0.0024 and ρ = 0.4632, P = 0.0147 for vaccine recipients at their peak immunogenicity timepoints after DDDMM or CCM, respectively; Extended Data Fig. 2a). Although the HTI magnitude

https://doi.org/10.1038/s41591-022-02060-2

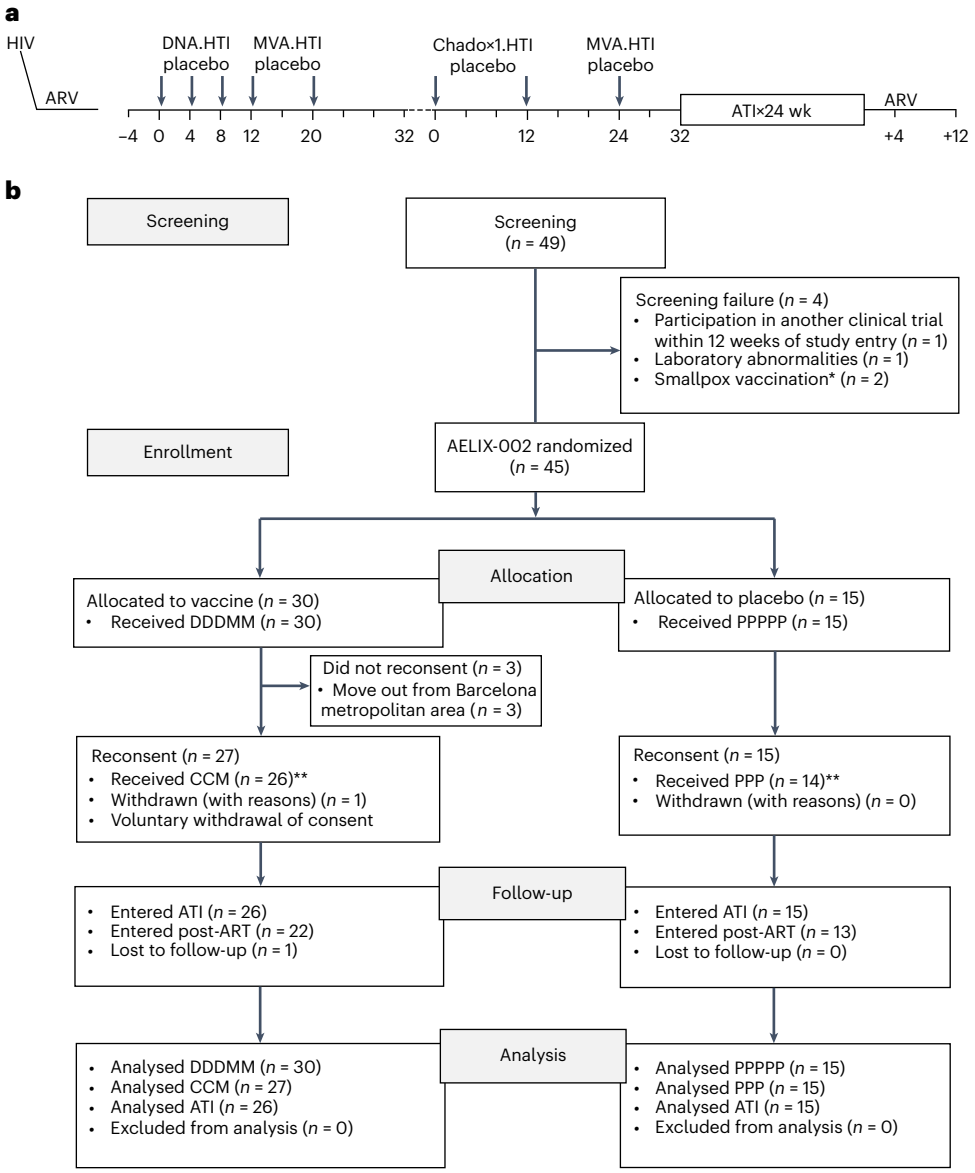

Fig. 1 | Trial design. a, Schematic trial design and study visits. **b**, Consolidated Standards of Reporting Trials (CONSORT) flow diagram for the trial. HIV, human immunodeficiency virus; ARV, antiretroviral therapy; ATI, analytical treatment interruption; D, DNA.HTI; M, MVA.HTI; C, ChAdOx1.HTI; P, placebo.

at the peak immunogenicity timepoint was higher after DDDMM in vaccinees with pre-ART HTI-specific responses compared to those without any HTI-detectable responses before ART initiation (median (range) of 2,203 (460–3,200) versus 808 (60–1,595) SFCs per million PBMCs, Mann–Whitney *t*-test, $P = 0.0380$), these differences were no longer statistically significant at ATI initiation (median (range) of 795 (165–2,705) versus 595 (50–980) SFCs per million PBMCs, Mann–Whitney *t*-test, $P = 0.1012$; Extended Data Fig. 2b). To determine whether HTI vaccination was able to shift the focus of the virus-specific T cells, the percentage of HTI-specific T-cell frequencies divided by the total HIV-1 proteome-specific T-cell frequencies was calculated at each timepoint. At the time of ATI start, the median (range) of 14% (0–50) versus 67% (0–100) of the total anti-HIV-1 T-cell response was HTI-specific in placebo and vaccine recipients, respectively (Mann–Whitney *t*-test $P < 0.001$; Fig. 2d).

To further characterize the vaccine-induced T cells, intracellular cytokine staining for IFN-γ, GranzymeB (GzmB), interleukin-2 (IL-2) and tumor necrosis factor-α (TNF-α) was performed in samples obtained four weeks after the last CCM or placebo vaccination (week 28) with or without in vitro stimulation with four different peptide pools covering the HTI immunogen. T-cell lineage, phenotype, activation and exhaustion surface markers were included in the panel. The results showed that HTI-specific responses, defined as the sum of the HTI-IFN-γ$^+$ populations for each of the four HTI peptide pool stimulations, were both CD4 and CD8 T-cell-mediated (Fig. 2e). Polyfunctionality analyses showed that, compared to placebo recipients, vaccinees had a higher frequency of bi and three-function CD8 T cells expressing IFN-γ/GzmB or IFN-γ/GzmB/TNF-α, whereas CD4 T cells predominantly expressed combinations of IL-2, IFN-γ and TNF-α (Fig. 2f). Importantly, and despite the intense vaccination regimen used in the study (DDDMM-CCM), T-cell exhaustion markers were not increased in HTI-specific T cells in vaccinees compared to placebo recipients after completing the last series of vaccination (Supplementary Table 5).

Finally, we measured the in vitro antiviral capacity of CD8$^+$ T cells by a standard viral inhibition assay (VIA)[17] using autologous CD4$^+$ T cells infected with two laboratory-adapted HIV-1 strains (BaL (R5 tropic virus) and IIIB (X4 tropic virus)) as well as with the autologous HIV virus. Median (interquartile range (IQR)) percentages of inhibition

https://doi.org/10.1038/s41591-022-02060-2

Table 1 | Study population

Demographics	Placebo, *n*=15	Vaccine, *n*=30	ITT population, *n*=45
Age, years	34 (20–51)	37 (23–57)	36 (20–57)
Sex at birth, male, *n* (%)	15 (100%)	29 (96.7%)	44 (97.8%)
BMI (kg m^{-2})	22.5 (19.1–31.7)	22.8 (19.1–32.2)	22.8 (19.1–32.2)
Time from estimated HIV transmission to ART initiation (days)	55 (12–125)	64 (6–140)	63 (6–140)
Fiebig stage at ART initiation, *n* (%)[a]			
I	1 (6.7%)	1 (3.3%)	2 (4.4%)
II	0 (0%)	2 (6.7%)	2 (4.4%)
III	2 (13.3%)	0 (0%)	2 (4.4%)
IV	0 (0%)	2 (6.7%)	2 (4.4%)
V	5 (33.3%)	19 (63.3%)	24 (53.3%)
VI	7 (46.7%)	6 (20%)	13 (28.9%)
pVL at ART initiation, log copies ml^{-1}	4.9 (3.7–7)	4.7 (2.9–7)	4.7 (2.9–7)
Current ART, *n* (%)			
DTG/ABC/3TC	7 (46.7%)	9 (30%)	16 (35.6%)
EVG/c/(TAF or TDF)/FTC	4 (26.7%)	13 (43.3%)	17 (37.8%)
RAL+ABC/3TC	1 (6.7%)	2 (6.7%)	3 (6.7%)
RAL+TDF/FTC	3 (20%)	6 (20%)	9 (20%)
Time with undetectable pVL (months)	18 (13–56)	27 (12–55)	24 (11–56)
Absolute CD4 (cells mm^{-3})	826 (549–2,156)	727 (457–1,333)	745 (365–2,156)
Percentage CD4 (%)	39.2 (19–53.9)	35.4 (17.8–63.4)	36.3 (17.8–63.4)
CD4/CD8 ratio	1.1 (0.5–2.66)	1.02 (0.5–3.3)	1 (0.5–3.3)
Beneficial HLA alleles any	3 (20%)	7(23.3%)	10 (22.2%)
B2705	1 (6.7%)	4 (13.3%)	5 (11.1%)
B5701	2 (13.3%)	1 (3.3%)	3 (6.7%)
B1517	0 (0%)	1 (3.3%)	1 (2.2%)
B1503	0 (0%)	1 (3.3%)	1 (2.2%)
Past smallpox vaccination[b]	1 (6.7%)	6 (20%)	7 (15.6%)
CCR5-Δ32 heterozygosity[c]	2 (13.3%)	3 (10%)	5 (11.1%)

Demographic, clinical and treatment characteristics of study participants at study entry (*n*=45). Data presented as median (min–max) except where specified. [a]According to Fiebig[37]. [b]Signs of scarification or history of vaccination reported by the volunteer. [c]CCR5-Δ32 genotype was available for 15 placebo and 26 vaccine recipients (those entering the ATI). Comparisons between study groups by two-sample *t*-test or chi-squared test when corresponding (non-significant for all variables). BMI, body mass index; ART, antiretroviral therapy; pVL, HIV-1 plasma viral load; DTG, dolutegravir; ABC, abacavir; 3TC, lamivudine; EVG/c, elvitegravir/cobicistat; TAF, tenofovir alafenamide fumarate; TDF, tenofovir disoproxil fumarate, ITT, intention-to-treat.

of the BaL-isolate increased in the vaccine group from 46(17; 75)% at baseline to 75(9; 88)% at the end of the intervention (Wilcoxon *t*-test, $P = 0.0805$), but it remained unchanged in the placebo group (34 (17; 60)% at baseline and 37 (14; 63)% at the end of the intervention (Wilcoxon *t*-test, $P = 0.9153$)). When using IIIB viruses and a participant's autologous viruses, significant changes in VIA were detected as well (Wilcoxon *t*-test, $P = 0.0014$ and 0.0176) in vaccinees in contrast to placebo recipients. However, absolute increases in viral inhibition capacity were of minor magnitude, probably due to the high inhibition capacity against the autologous virus already present at study entry, and consistent with early treatment initiation (Fig. 2g).

Effect on viral rebound during an ATI

Of the participants, 41 (15 placebo and 26 vaccine recipients) interrupted ART and were monitored weekly for a maximum of 24 weeks. Criteria for ART resumption included a single HIV-1 plasma viral load (pVL) of >100,000 copies ml^{-1}, eight consecutive determinations of >10,000 copies ml^{-1}, two repeated CD4$^+$ cell counts of <350 cells mm^{-3} and/or development of grade 3 or higher-severity clinical symptoms suggestive of an acute retroviral syndrome (ARS)—whichever appeared first. The ATI period partially overlapped with the first COVID-19 outbreak in Spain, with a State of Alarm declared from 16 March 2020 to 20 June 2020. Risk mitigation strategies were quickly implemented during the pandemic to reduce premature withdrawals while ensuring participants' safety. ATI was tolerated well overall (Supplementary Table 6). The frequency of sexually transmitted infections (STIs) in the study population was similar to those previously reported in MSM (men who have sex with other men)[18], but importantly was relatively lower during the ATI period than during the intervention phase of the study (7 versus 17 cases of STI per 100 persons per year, respectively). Viral suppression to undetectable levels was achieved by the 12th week after ART resumption in all 35 participants assessed at the end-of-study visit.

As shown in Fig. 3a,b, pVL rebound (defined as pVL > 50 copies ml^{-1}) was detected in all 41 participants after ART discontinuation at a median (range) time of 2 (1–6) and 3 (1–9) weeks in placebo and vaccine recipients, respectively (Mann–Whitney *t*-test, $P = 0.1942$). Time to pVL rebound, peak viremia, time to peak viremia, slope of increasing pVL or area under the curve (AUC) pVL during the ATI were comparable between placebo and vaccine recipients (Extended Data Table 4). Of the participants, 25 (61%) resumed ART after one determination of pVL > 100,000 copies ml^{-1}, and one (2%) participant after eight consecutive determinations of >10,000 copies ml^{-1}. Three participants (one in the placebo and two in the vaccine group) showed symptoms compatible with ARS, but they were grade 1–2 and did not proceed to ART resumption. Four (9%) participants resumed ART at weeks 9, 12, 22 and 23 of ATI without reaching any pre-specified ART resumption criteria in the context of the COVID-19 pandemic (details are provided in Supplementary Table 7). Eleven (27%) participants completed 24 weeks of ATI, seven of them with sustained pVL < 2,000 copies ml^{-1}. Five participants resumed ART at week 24, and the remaining six participants (two placebo and four vaccine recipients) opted to remain off ART and entered an ATI-extension protocol with monthly monitoring for up to a total of 72 weeks of ATI (NCT04385875). Four participants (one placebo and three vaccine recipients) completed the ATI extension with sustained pVL < 2,000 copies ml^{-1} after 72 weeks off ART (Extended Data Fig. 3), and then resumed ART. Reasons for starting ART included worries about HIV transmission, previous good tolerability to ART and the burden of additional HIV prevention tools required for viremic individuals. In a post-hoc survival analysis for time off ART during the ATI, participants without any beneficial HLA class I alleles (32 of the 41 participants that entered the ATI period), one (8%) of the placebo and eight (40%) of the vaccine recipients were able to remain off ART for 22 weeks (Δ 32%, 80% confidence interval (CI) (7.6; 55.7) and 95% CI (−1.6; 64.9); log-rank test $P = 0.1834$ for all ATI), with pVL < 2,000 copies ml^{-1} being observed in one placebo and five vaccine recipients, respectively (Fig. 3c)

Exploratory objectives

Reservoir. Amplicon signal issues occurred for six (14%) participants (three placebo and three vaccine recipients) for whom intact proviral DNA assay (IPDA) determinations were not available. Intact HIV-1 DNA represented a median (IQR) of 23% (9; 42) of the total HIV-1 DNA. Total and intact proviral HIV-1 DNA were highly correlated (Spearman's $\rho = 0.6673$, $P < 0.0001$ at study entry and $\rho = 0.8716$, $P < 0.0001$ at ATI

start). No differences in reservoir decay were found between groups, either measured by total proviral HIV-1 DNA (21% versus 16% decay in the placebo and vaccine groups, respectively, Wilcoxon *t*-test, $P = 0.4291$) or by IPDA (68% versus 66% decay in the placebo and vaccine groups, respectively, Wilcoxon *t*-test, $P = 0.7892$) (Extended Data Fig. 4).

Correlate analyses. Potential immune and viral correlates associated with longer time off ART (that is, less risk to reach the ART resumption criteria of HIV-1 pVL > 100,000 or consecutive HIV-1 pVL > 10,000 for more than eight weeks) were assessed in the subgroup of individuals that did not harbor any HLA class I allele associated with spontaneous HIV control. The magnitude of the HTI-specific T-cell response at ATI start was significantly associated with both prolonged time off ART and with lower pVL at the end of ATI in vaccinees (Spearman's $\rho = 0.6469$, $P = 0.0021$ and $\rho = -0.6837$, $P = 0.0009$, respectively; Fig. 4a,b) but not in placebo recipients. Similarly (albeit not statistically significant), the cumulative breadth of HTI-specific responses at ATI start was associated with longer time off ART (Spearman's $\rho = 0.4235$, $P = 0.0628$; Supplementary Fig. 1). In terms of specificities within HTI, for those vaccinees remaining off ART for longer than 12 weeks ($n = 8$), we did not observe differences in the pattern of responses induced across the different HIV protein segments covered by HTI (Supplementary Fig. 1).

As for T-cell functionality, the frequency of $CD8^+$—and to a lesser extent $CD4^+$—T cells expressing $GzmB^+$ was positively correlated with time off ART and with lower HIV-1 pVL at the end of ATI in vaccine, but not in placebo recipients (Fig. 4c–f). Although vaccinees showed an increase in in vitro viral inhibition capacity, this was not associated with any of the ATI outcomes. As for viral factors, we ruled out the possibility that pre-existing CTL escape in sequences covered by HTI immunogen and/or replication fitness of the participants' autologous virus could have influenced the ability of vaccine-induced responses to control virus replication during ATI. Vaccine recipients that remained off ART for longer periods of time did not show any significant correlation with the number of HLA-adapted footprints in pre-ART sequences (Spearman's $\rho = -0.0160$, $P = 0.9467$; Extended Data Fig. 5a) and were able to control viruses not only with low but also with medium and high replicative capacity (Extended Data Fig. 5b). Levels of total or intact proviral HIV-1 DNA at ATI start were not associated with time to viral rebound or with longer time off ART (Extended Data Fig. 5c,d). However, the majority of participants that remained off ART for >12 weeks were among those with lower reservoir levels.

Finally, as the distribution of time off ART was quite binary rather than continuous (≤12 or >12 weeks), univariate logistic regression models were used to identify factors that could influence length of time to ART resumption. In addition to the pre-ART pVL, most of the immune parameters measured at ATI start increased the odds of time off ART > 12 weeks (for example, HTI magnitude $\widehat{OR}$ (odds ratio) 1.46, 95% CI (1.16; 1.99), $P = 0.0052$; frequency of HTI-specific $CD8^+$ $GzmB^+$ T cells at ATI start $\widehat{OR}$ 1.07, 95% CI (1.01; 1.14), $P = 0.0240$; Fig. 5). Conversely, reservoir levels were not associated with higher chances of remaining off ART in the regression model. Importantly, in a multivariate logistic regression model including most critical demographic covariates, such as pre-ART pVL and CD4/CD8 ratio at AELIX-002 entry, there was an increased probability for being off ART after 12 weeks of ATI for the vaccinees compared to placebo recipients ($\widehat{OR}$ 8.25, 95% CI (1.05; 140.36); Extended Data Table 5).

Discussion

The double-blind, placebo-controlled, randomized AELIX-002 study has demonstrated that HTI vaccines were safe, well-tolerated and able to induce strong, polyfunctional and broad CD4 and CD8 T-cell responses focused on the HTI immunogen sequence. In agreement with preclinical data in NHP (non-human primates)[19] and clinical trials in similar populations using other T-cell vaccines only[5,6], all participants showed detectable viral rebound during the ATI. However, in exploratory analyses we observed a positive efficacy signal on the ability to remain off ART during a 24-week ATI (that is, to avoid reaching an HIV-1 pVL of >100,000 copies ml^{-1} or >10,000 copies ml^{-1} for eight consecutive weeks as per the protocol-defined ART resumption criteria) in vaccinees without beneficial HLA genetics compared to placebo recipients. The AELIX-002 trial is a randomized, placebo-controlled trial testing therapeutic T-cell vaccines in an early ART-treated population that shows a correlation between vaccine-induced immune responses and both lower post-rebound viremia and extended time off ART, providing an opportunity to identify correlates of improved viral control.

The AELIX-002 trial results support the idea that the induction of HIV-specific T cells is a key factor in improving post-rebound viral suppression during an ATI, while validating the design of the HTI immunogen to induce functional T-cell responses to vulnerable sites of the virus. Indeed, the HTI vaccines used in AELIX-002 showed good coverage of the autologous viral sequences, despite some evidence of pre-existing CTL escape[20]. Importantly, HTI vaccination induced strong, long-lasting GzmB-secreting $CD8^+$ T cells along with an improved ability to inhibit replication of CCR5-tropic, CXCR4-tropic and, importantly, autologous HIV virus with a broad range of viral replicative fitness. Additionally, vaccine-induced responses targeted different HTI subunits, confirming that the HTI immunogen design does contain multiple T-cell targets that can mediate effective HIV control ex vivo.

Studies testing a combination of TLR7 agonists and bNAbs in NHP have observed a correlation between lower pre-ART pVL in acute infection and time to viral rebound during an ATI[21]. In contrast, in

Fig. 2 | Vaccine immunogenicity. a, Magnitude (sum of SFCs per 10^6 PBMCs for HTI pools P1–P10) over the AELIX-002 study in placebo (blue) and vaccine (red) recipients over the two vaccination regimens (DDDMM/PPPPP and CCM/PPP) up to the start of the ATI period. **b**, Breadth of vaccine-elicited responses towards individual OLPs spanning the entire HTI sequence in the 15 placebo and 30 vaccine recipients. Boxplots represent the median and IQR, and the *P* values correspond to comparisons between the indicated timepoints using the Wilcoxon signed-rank test. **c**, Distribution of HTI-specific responses within the different HIV-1 subproteins included in the HTI immunogen of cumulative breadth at AELIX-002 study entry (top) and after completion of the last series of vaccinations (bottom) for each placebo (P1 to P15) and vaccine (V1 to V26) recipient. **d**, Average distribution of total HIV-1 T cells according to their specificity at the indicated timepoints. HTI-specific responses are shown for placebo (blue) and vaccine (red) recipients. The other non-HTI HIV-1 specific responses are shown in gray. *P* values correspond to a comparison between the proportion of HTI-specific responses at each timepoint. Fisher's exact test is used for comparisons between groups. **e**, Proportion of HTI-specific $CD4^+$ and $CD8^+$ T cells secreting IFN-γ (left) or both IFN-γ and GzmB (right) after completion of the last series of HTI vaccinations (DDDMM-CCM/PPPP-PPP). Data are presented as median and IQR for the sum of IFN-γ^+ and IFN-γ^+/$GzmB^+$ for each of the four HTI peptide pool stimulations. A Wilcoxon–Mann–Whitney test is used for comparison between placebo ($n = 12$) and vaccine ($n = 20$) groups. **f**, Polyfunctionality of HTI-specific $CD4^+$ and $CD8^+$ T cells analyzed by Boolean gating. Pie charts and boxplots per treatment group (placebo $n = 15$, vaccine $n = 26$) illustrate the relative and absolute proportion of each of the different subsets (cells producing two, three or four cytokines), respectively. On each boxplot, the central line indicates the median, and the bottom and top edges of the box indicate the 25th and 75th percentiles, respectively. The whiskers extend to 1.5 times the IQR. *P*-values correspond to the Mann–Whitney test per row, adjusted for multiple comparisons. **g**, Changes in viral inhibition capacity to laboratory-adapted HIV-1 strains (placebo $n = 15$, vaccine $n = 26$) and autologous HIV-1 (placebo $n = 14$, vaccine $n = 23$) at study entry, after DDDMM/PPPPP and CCM/PPP regimens for placebo (blue) and vaccine (red) recipients. Boxplots represent median and IQR, and the *P* values correspond to comparisons between the indicated timepoints using the Wilcoxon signed-rank test. SCR, screening; BSL, baseline; D, DNA.HTI; M, MVA.HTI; C, ChAdOx1.HTI; P, placebo.

https://doi.org/10.1038/s41591-022-02060-2

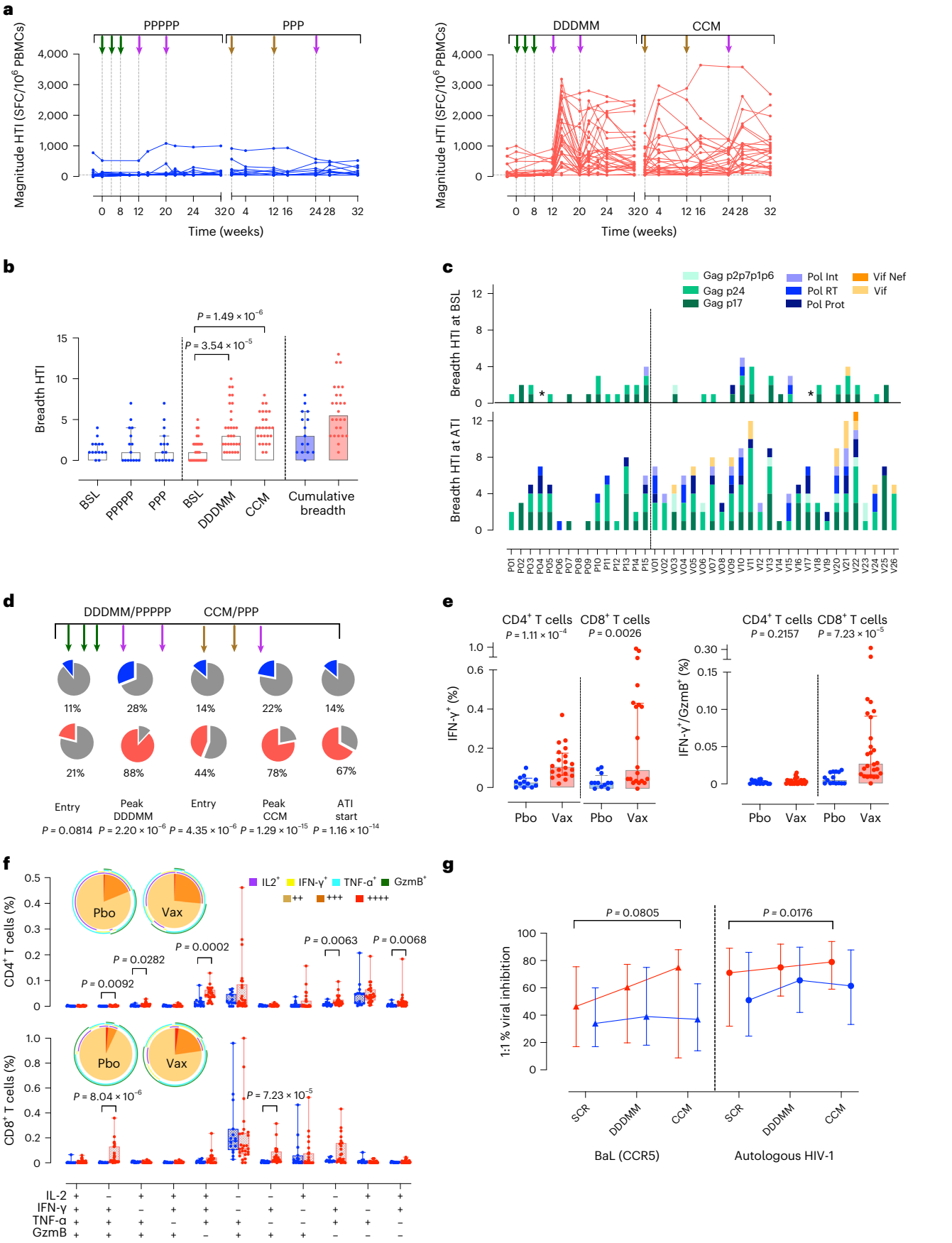

https://doi.org/10.1038/s41591-022-02060-2

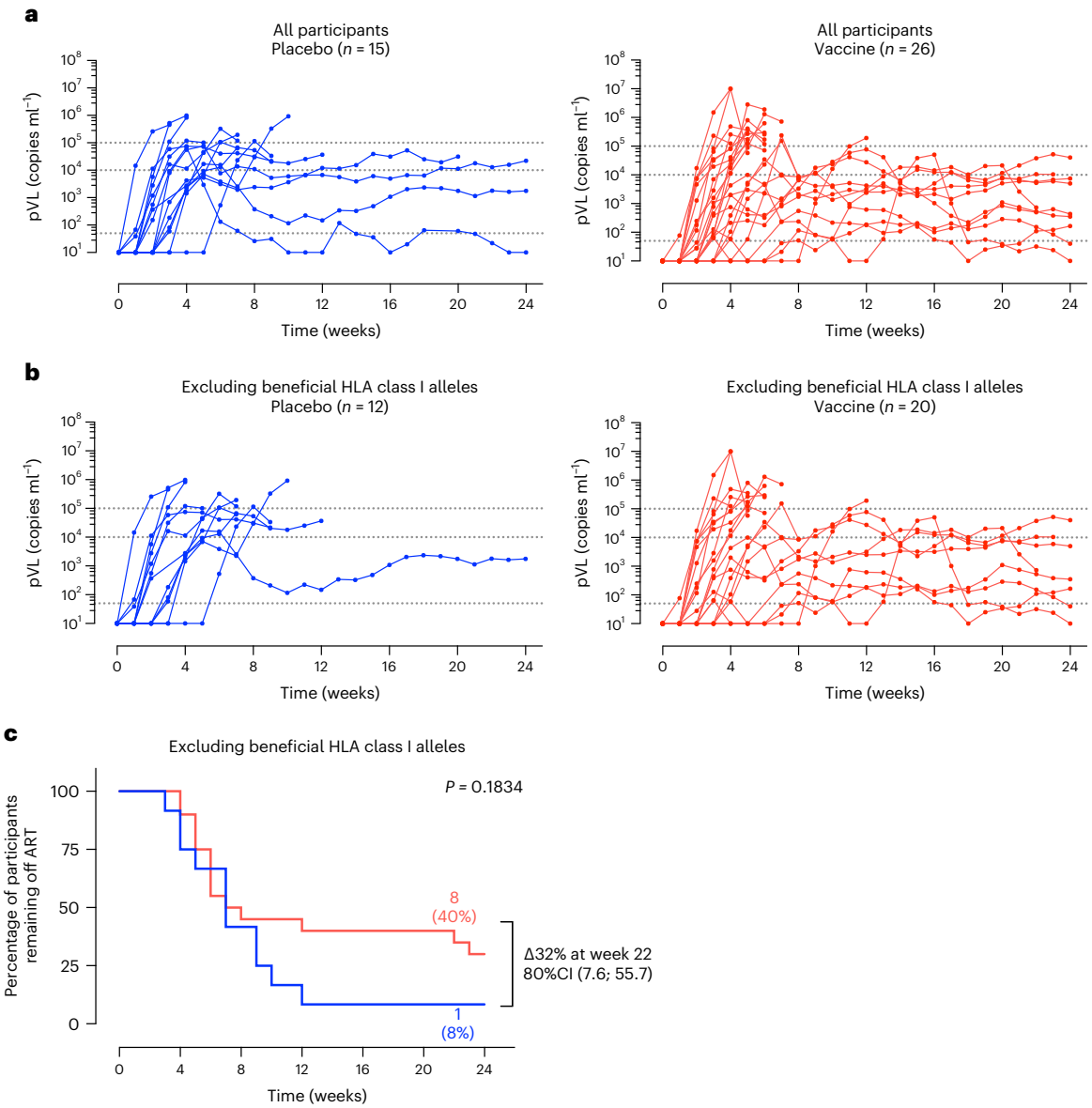

Fig. 3 | ATI period. a,**b**, Individual HIV-1 pVL during the 24 weeks of ATI, shown for all placebo (blue) or vaccine (red) recipients (**a**) and in those without any beneficial HLA associated with spontaneous viral control (**b**). Lines are interrupted at the week of ART resumption. Dotted lines represent the detection limit and the two different virologic thresholds for ART resumption (10,000 and 100,000 HIV-1 RNA copies per ml, respectively). **c**, Proportion of participants without any beneficial HLA allele associated with spontaneous viral control in the placebo and vaccine arms remaining off ART following treatment interruption. The log-rank test is used for comparison between groups over the entire ATI period. The proportion of participants, delta and 80% CI are shown for week 22 of ATI, before the last two vaccine recipients resumed ART for COVID-19-related reasons without fulfilling any per-protocol virological criteria. pVL, plasma viral load; ART, antiretroviral treatment.

AELIX-002, lower pre-ART pVL was not associated with longer time to first detectable pVL during the ATI, but it was positively correlated with time off ART. Importantly, in exploratory multivariate models, the association of vaccination with extended time off ART remained statistically significant, even after accounting for participants' levels of pre-ART viremia and CD4/CD8 ratio.

Different approaches have been developed to establish high-throughput assays to quantify the replication-competent viral reservoir relevant for cure-related trials, including the IPDA assay, which allows measurement of genetically intact proviruses and excludes the majority of defective proviruses[22,23]. In AELIX-002, although the intact proviral HIV-1 DNA declined preferentially over time relative to total proviruses, we did not detect differences in the reservoir decay from baseline to ATI associated with therapeutic vaccination, suggesting that such a reduction reflected natural decay curves due to early treatment[15]. In contrast to others who have reported an association between a delay in viral rebound and lower intact proviral DNA levels after vesatolimod treatment in viremic controllers[24], we did not detect any correlation between levels of intact proviral DNA and time to viral rebound in our early-treated population. Of note, seven (17%) participants that entered the ATI period had no detectable levels of intact HIV-1 proviruses at the time of ART cessation and yet experienced viral rebound during the ATI.

Despite the extended vaccination regimen used in AELIX-002, vaccinations were safe and well-tolerated, and safety profiles were comparable to other HIV vaccines using the same vector platforms both in HIV-negative[25] or HIV-positive individuals[2]. No serious related AEs or laboratory abnormalities were observed after either DDDMM or CCM vaccinations, including any suspected vaccine-induced immune thrombotic

https://doi.org/10.1038/s41591-022-02060-2

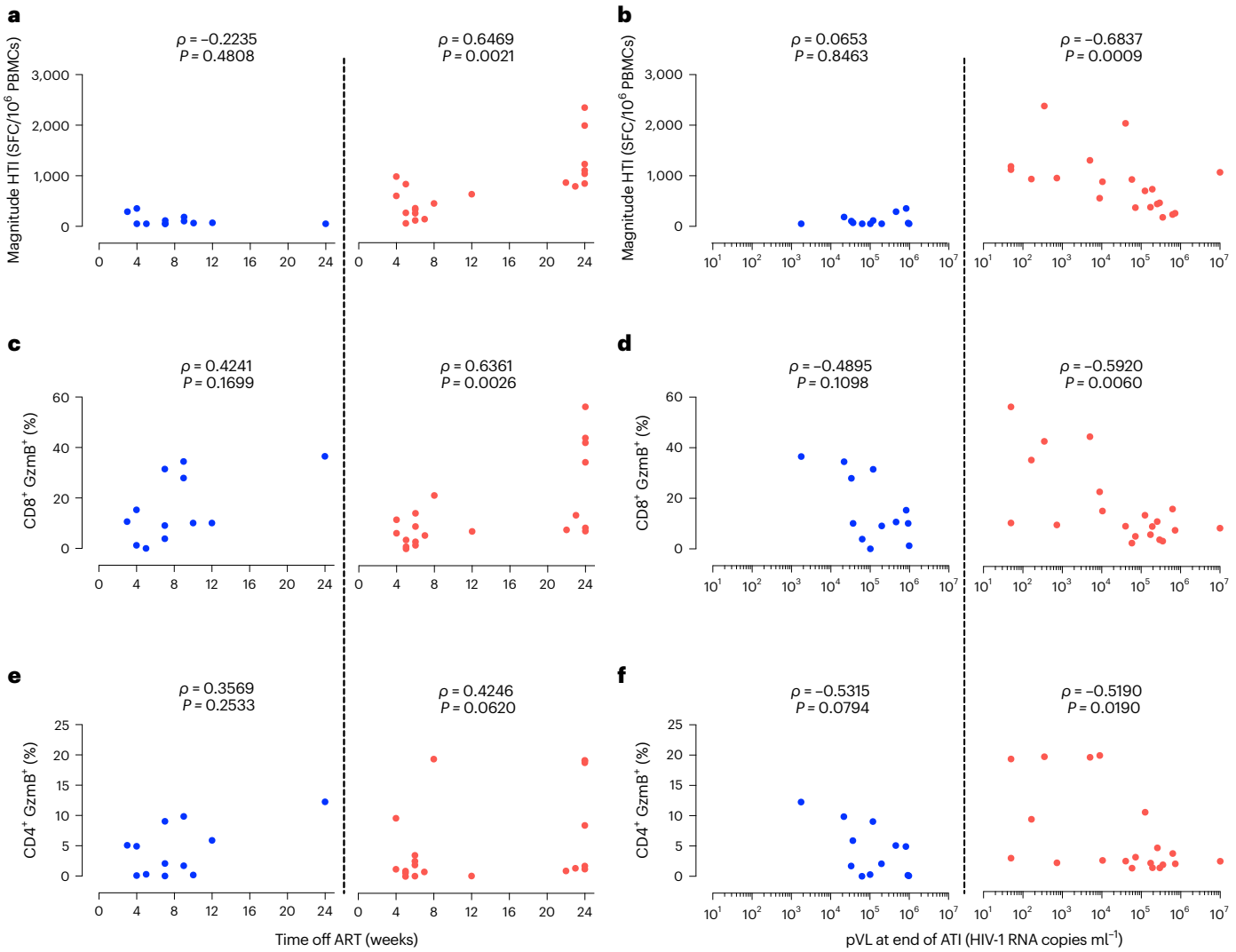

Fig. 4 | Immune correlates with ATI outcomes in participants without any beneficial HLA allele. a–**f**, Correlation between time off ART (left) and HIV-1 pVL at the end of ATI at the ART resumption timepoint (right) for HTI magnitude at ATI start (**a**,**b**) and proportion of $CD8^+$ (**c**,**d**) and $CD4^+$ (**e**,**f**) GzmB-secreting T cells in placebo (blue) and vaccine (red) recipients. Spearman's correlation is used. ART, antiretroviral treatment; pVL, plasma viral load; ATI, analytical treatment interruption.

thrombocytopenia (VITT), as described for ChAdOx1-vectored COVID-19 vaccines[26]; although our sample size was rather limited to detect such rare events. Notewothy, T-cell exhaustion markers were not increased in vaccinees compared to placebo recipients.

Similar to the ATI viral kinetics in the AELIX-002 trial, in which all participants experienced a fast viral rebound, Okoye et al. have recently shown in the NHP model that $CD8^+$ T cells contribute to reduce the viral set point, although they were not able to prevent viral recrudescence[19]. These data suggest that HIV antigenic stimulation might be necessary to trigger an effective immune response during the ATI. This, in turn, has important implications for the design of ATI trials where ART resumption criteria may need to be permissive enough to allow for such a transient viremia[27–29]. Initial peak viremia may, however, also be associated with risks for onward virus transmission, mutational T-cell escape, reseeding of the viral reservoir and/or excessive inflammatory responses giving rise to ARS. Therefore, it is critical to balance research objectives and the well-being of participants while considering, in collaboration with community advisory boards, effective transmission risk-reduction strategies[30]. In AELIX-002, ART resumption criteria during the ATI were well-accepted among participants, as well as all transmission-risk reduction strategies implemented, which included PrEP provision to sexual partners, psychological support and active surveillance for asymptomatic STI. Of note, the AELIX-002 study, and the ATI phase in particular, was ongoing when the first COVID-19 outbreak occurred in Spain. This severely impacted many clinical trial sites, as most non-COVID-related hospital activities, including clinical research, had to be paused. Rapid establishment of a risk-mitigation plan overseen by an external SMC during the emergency outbreak was critical to minimize the impact of the COVID-19 pandemic on the conduct of AELIX-002, as some investigators have recommended recently[31,32].

The main limitations of our trial include the sample size, which did not allow for a powered subgroup analysis in individuals without beneficial HLA genetics, as well as the selected study population, which limited extrapolation of our results to HIV populations other than those treated early during acute/recent HIV infection and in which both cis-gender and transgender women are usually underrepresented. In addition, the regimen used in AELIX-002 consisted of two different vaccination regimens of DDDMM, further boosted by CCM vaccines; overall, this does not represent a clinically feasible vaccination regimen, but it did serve to set up an efficacy proof of concept of the HTI immunogen design. In fact, we acknowledge that the efficacy endpoint of time off ART in our study is a function of the ART resumption criteria

https://doi.org/10.1038/s41591-022-02060-2

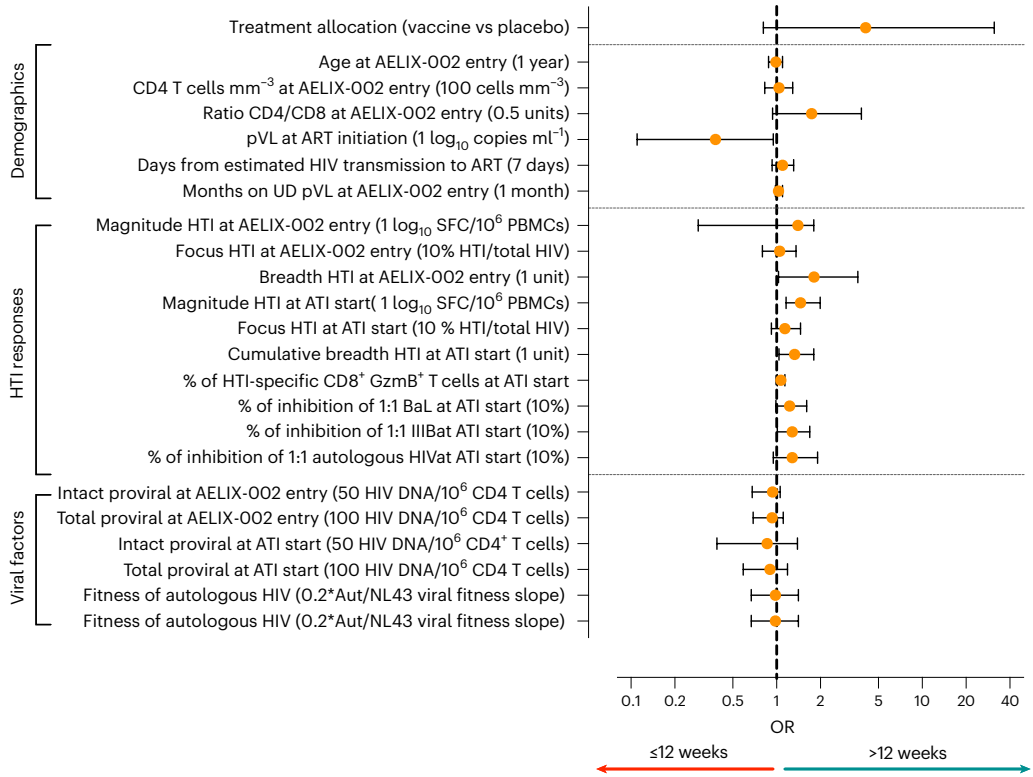

Fig. 5 | Univariate correlate analysis. Odds ratio and its 95% CI of time to ART resumption >12 weeks in univariate logistic regression models (n = 32 participants without beneficial alleles).

used in the protocol and, importantly, is not yet translatable into clinical practice.

Our findings strongly support the further use of HTI vaccines in simpler regimens, given alone or in combination with other immunomodulatory agents to improve their efficacy, to achieve more clinically relevant virological outcomes and to be better aligned with the most current target product profile for an HIV cure indication[33]. For example, to avoid viral rebound, or partially curtail fast and severe viral recrudesence, and to improve the level of virus control, we and others have proposed strategies combining therapeutic vaccines with bNAbs, which at the same time may enhance suppressive capacity of vaccine-induced responses through a vaccinal effect[34–36]. In this sense, the BCN03 and AELIX-003 clinical trials (NCT05208125 and NCT04364035, respectively) are currently exploring the safety and immunogenicity of a ChAdOx1.HTI/MVA.HTI vaccine regimen with a recombinant HIV-1 envelope SOSIP protein (ConM SOSIP.v7 gp140) or with a TLR7 agonist (vesatolimod) including an ATI with the same ART resumption criteria as in AELIX-002.

In conclusion, this first administration of a heterologous prime-boost regimen of HTI vaccines in early ART-treated individuals with HIV infection was safe and immunogenic. In exploratory analyses, AELIX-002 showed a potential signal for improved post-rebound viral control after ART discontinuation in a subset of individuals who did not already possess a beneficial HLA genotype; this requires validation in future studies. These data provide support for the use of HTI vaccines as a T-cell-stimulating backbone for future combination cure strategies, with the addition of immunomodulators, bNAbs or alternative vaccine vectors to boost their efficacy.

Online content

Any methods, additional references, Nature Research reporting summaries, source data, extended data, supplementary information, acknowledgements, peer review information; details of author contributions and competing interests; and statements of data and code availability are available at https://doi.org/10.1038/s41591-022-02060-2.

References

1. Shan, L. et al. Stimulation of HIV-1-specific cytolytic T lymphocytes facilitates elimination of latent viral reservoir after virus reactivation. *Immunity* **36**, 491–501 (2012).
2. Mothe, B. et al. Therapeutic vaccination refocuses T-cell responses towards conserved regions of HIV-1 in early treated individuals (BCN 01 study). *EClinicalMedicine* **11**, 65–80 (2019).
3. Mothe, B. et al. HIVconsv vaccines and romidepsin in early-treated HIV-1-infected individuals: safety, immunogenicity and effect on the viral reservoir (Study BCN02). *Front. Immunol.* **11**, 823 (2020).
4. Fidler, S. et al. Antiretroviral therapy alone versus antiretroviral therapy with a kick and kill approach, on measures of the HIV reservoir in participants with recent HIV infection (the RIVER trial): a phase 2, randomised trial. *Lancet* **395**, 888–898 (2020).
5. Colby, D. J. et al. Safety and immunogenicity of Ad26 and MVA vaccines in acutely treated HIV and effect on viral rebound after antiretroviral therapy interruption. *Nat. Med.* **26**, 498–501 (2020).
6. Sneller, M. C. et al. A randomized controlled safety/efficacy trial of therapeutic vaccination in HIV-infected individuals who initiated antiretroviral therapy early in infection. *Sci. Transl. Med.* **9**, eaan8848 (2017).
7. Søgaard, O. S. et al. The depsipeptide romidepsin reverses HIV-1 latency in vivo. *PLoS Pathog.* **11**, e1005142 (2015).
8. Mothe, B. et al. Definition of the viral targets of protective HIV-1-specific T cell responses. *J. Transl. Med.* **9**, 208 (2011).
9. Mothe, B. et al. A human immune data-informed vaccine concept elicits strong and broad T-cell specificities associated with HIV-1 control in mice and macaques. *J. Transl. Med.* **13**, 60 (2015).

10. Mothe, B. et al. CTL responses of high functional avidity and broad variant cross-reactivity are associated with HIV control. *PLoS ONE* **7**, e29717 (2012).
11. Hancock, G. et al. Identification of effective subdominant anti-HIV-1 CD8$^+$ T cells within entire post-infection and post-vaccination immune responses. *PLoS Pathog.* **11**, e1004658 (2015).
12. Kulkarni, V. et al. Comparison of immune responses generated by optimized DNA vaccination against SIV antigens in mice and macaques. *Vaccine* **29**, 6742–6754 (2011).
13. Létourneau, S. et al. Design and pre-clinical evaluation of a universal HIV-1 vaccine. *PLoS ONE* **2**, e984 (2007).
14. Dicks, M. D. J. et al. A novel chimpanzee adenovirus vector with low human seroprevalence: improved systems for vector derivation and comparative immunogenicity. *PLoS ONE* **7**, e40385 (2012).
15. Bayón-Gil, Á. et al. HIV-1 DNA decay dynamics in early treated individuals: practical considerations for clinical trial design. *J. Antimicrob. Chemother.* **75**, 2258–2263 (2020).
16. Goulder, P. J. R. & Walker, B. D. HIV and HLA Class I: an evolving relationship. *Immunity* https://doi.org/10.1016/j.immuni.2012.09.005 (2012).
17. Yang, H. et al. Antiviral inhibitory capacity of CD8$^+$ T cells predicts the rate of CD4$^+$ T-cell decline in HIV-1 infection. *J. Infect. Dis.* **206**, 552–561 (2012).
18. Werner, R. N., Gaskins, M., Nast, A. & Dressler, C. Incidence of sexually transmitted infections in men who have sex with men and who are at substantial risk of HIV infection—a meta-analysis of data from trials and observational studies of HIV pre-exposure prophylaxis. *PLoS ONE* **13**, e0208107 (2018).
19. Okoye, A. A. et al. CD8$^+$ T cells fail to limit SIV reactivation following ART withdrawal until after viral amplification. *J. Clin. Invest.* **131**, e141677 (2021).
20. Deng, K. et al. Broad CTL response is required to clear latent HIV-1 due to dominance of escape mutations. *Nature* **517**, 381–385 (2015).
21. Borducchi, E. N. et al. Antibody and TLR7 agonist delay viral rebound in SHIV-infected monkeys. *Nature* **563**, 360–364 (2018).
22. Gaebler, C. et al. Sequence evaluation and comparative analysis of novel assays for intact proviral HIV-1 DNA. *J. Virol.* **95**, e01986920 (2021).
23. M, A.-M. et al. Recommendations for measuring HIV reservoir size in cure-directed clinical trials. *Nat. Med.* **26**, 1339–1350 (2020).
24. SenGupta, D. et al. The TLR7 agonist vesatolimod induced a modest delay in viral rebound in HIV controllers after cessation of antiretroviral therapy. *Sci. Transl. Med.* **13**, eabg3071 (2021).
25. Hayton, E.-J. et al. Safety and tolerability of conserved region vaccines vectored by plasmid DNA, simian adenovirus and modified vaccinia virus ankara administered to human immunodeficiency virus type 1-uninfected adults in a randomized, single-blind phase I trial. *PLoS ONE* **9**, e101591 (2014).
26. Greinacher, A. et al. Thrombotic thrombocytopenia after ChAdOx1 nCov-19 vaccination. *N. Engl. J. Med.* **384**, 2092–2101 (2021).
27. Namazi, G. et al. The Control of HIV after Antiretroviral Medication Pause (CHAMP) study: post-treatment controllers identified from 14 clinical studies. *J. Infect. Dis.* https://doi.org/10.1093/infdis/jiy479 (2018).
28. Julg, B. et al. Recommendations for analytical antiretroviral treatment interruptions in HIV research trials—report of a consensus meeting. *Lancet HIV* **6**, e259–e268 (2019).
29. Fajnzylber, J. M. et al. Frequency of post treatment control varies by ART restart and viral load criteria. *AIDS* **35**, 2225–2227 (2021).
30. Dubé, K. et al. Ethical and practical considerations for mitigating risks to sexual partners during analytical treatment interruptions in HIV cure-related research. *HIV Res. Clin. Pract.* **22**, 14–30 (2021).
31. Peluso, M. J. et al. Operationalizing HIV cure-related trials with analytic treatment interruptions during the SARS-CoV-2 pandemic: a collaborative approach. *Clin. Infect. Dis. Publ. Infect. Dis. Soc. Am.* **72**, 1843–1849 (2021).
32. Fidler, S. et al. HIV cure research in the time of COVID-19—antiretroviral therapy treatment interruption trials: a discussion paper. *J. Virus Erad.* **7**, 100025 (2021).
33. Lewin, S. R. et al. Multi-stakeholder consensus on a target product profile for an HIV cure. *Lancet HIV* **8**, e42–e50 (2021).
34. Nishimura, Y. et al. Early antibody therapy can induce long-lasting immunity to SHIV. *Nature* **543**, 559–563 (2017).
35. Mendoza, P. et al. Combination therapy with anti-HIV-1 antibodies maintains viral suppression. *Nature* **561**, 479–484 (2018).
36. Caskey, M. Broadly neutralizing antibodies for the treatment and prevention of HIV infection. *Curr. Opin. HIV AIDS* **15**, 49–55 (2020).
37. Fiebig, E. W. et al. Dynamics of HIV viremia and antibody seroconversion in plasma donors: implications for diagnosis and staging of primary HIV infection. *AIDS* **17**, 1871–1879 (2003).

Lucia Bailón[1,2], Anuska Llano[3], Samandhy Cedeño[3], Tuixent Escribà[3], Miriam Rosás-Umbert[3,4], Mariona Parera[3], Maria Casadellà[3], Miriam Lopez[1], Francisco Pérez[1], Bruna Oriol-Tordera[3], Marta Ruiz-Riol[3,5], Josep Coll[3,5,6], Felix Perez[6], Àngel Rivero[6], Anne R. Leselbaum[6], Ian McGowan[7,8], Devi Sengupta[9], Edmund G. Wee[10], Tomáš Hanke[10,11], Roger Paredes[3,5,12,13], Yovaninna Alarcón-Soto[1,14], Bonaventura Clotet[1,3,5,12], Marc Noguera-Julian[3,5,12], Christian Brander[3,5,7,12,15,16], Jose Molto[1,5,13,16] ✉, Beatriz Mothe[1,3,5,12,13,16] and the AELIX002 Study Group[*]

[1]Fundació Lluita Contra les Infeccions, Infectious Diseases Department, Hospital Universitari Germans Trias I Pujol, Badalona, Barcelona, Spain. [2]Department of Medicine, Autonomous University of Barcelona, Catalonia, Spain. [3]IrsiCaixa AIDS Research Institute, Hospital Universitari Germans Trias I Pujol, Badalona, Barcelona, Spain. [4]Institute of Clinical Medicine, Aarhus University, Aarhus, Denmark. [5]CIBERINFEC, ISCIII, Madrid, Spain. [6]Projecte Dels Noms-Hispanosida, Bcn Checkpoint, Barcelona, Spain. [7]AELIX Therapeutics S.L, Barcelona, Spain. [8]University of Pittsburgh, Pittsburgh, PA, USA. [9]Gilead Sciences, Inc, Foster City, CA, USA. [10]The Jenner Institute, The Nuffield Department of Medicine, University of Oxford, Oxford, UK. [11]Joint Research Center for Human Retrovirus Infection, Kumamoto University, Kumamoto, Japan. [12]Centre for Health and Social Care Research (CESS), Faculty of Medicine. University of Vic – Central University of Catalonia (UVic – UCC), Vic, Barcelona, Spain. [13]Germans Trias I Pujol Research Institte, Badalona, Spain. [14]Departament d'Estadística I Investigació Operativa, Universitat Politècnica de Catalunya/BARCELONATECH, Barcelona, Spain. [15]ICREA, Barcelona, Spain. [16]These authors contributed equally: Christian Brander, José Moltó, Beatriz Mothe. *A list of authors and their affiliations appears at the end of the paper. ✉e-mail: jmolto@lluita.org

the AELIX002 Study Group

Yovaninna Alarcón-Soto[1,14], Lucia Bailón[1,2], Ana María Barriocanal[13], Susana Benet[1], Christian Brander[3,5,7,12,15,16], Maria Casadellà[3], Samandhy Cedeño[3], Bonaventura Clotet[1,3,5,12], Patricia Cobarsi[1], Josep Coll[3,5,6], Tuixent Escribà[3], Romas Geleziunas[9], Tomáš Hanke[10,11], Anne R. Leselbaum[7], Cora Loste[1], Miriam Lopez[1], Anuska Llano[3], Michael Meulbroek[6], Ian McGowan[7,8], Cristina Miranda[1], Jose Molto[1,5,13,16], Beatriz Mothe[1,3,5,12,13,16], Jose Muñoz[1], Jordi Naval[7], Aroa Nieto[1], Marc Noguera-Julian[3,5,12], Roger Paredes[3,5,12,13], Mariona Parera[3], Felix Perez[6], Ferran Pujol[6], Jordi Puig[1], Àngel Rivero[6], Miriam Rosás-Umbert[3,4], Marta Ruiz-Riol[3,5], Devi Sengupta[9], Bruna Oriol-Tordera[3] and Edmund G. Wee[10]

A list of members and their affiliations appears in the Supplementary Information.

Methods

Study design

AELIX-002 (clinicaltrials.gov NCT03204617) enrolled 45 HIV-positive early-treated individuals at the Infectious Diseases Department of the Hospital Germans Trias i Pujol (HUGTIP), Badalona, Spain. The first and last participants were recruited on 20 July 2017 and 5 June 2018, respectively. The last study visit was conducted on 10 March 2021. AELIX-002 was a phase I, proof-of-concept, first-in-human, randomized, double-blind, placebo-controlled study to evaluate the safety, immunogenicity and effect on viral rebound during an ATI of three novel HIV-1 vaccines (DNA.HTI (D), MVA.HTI (M) and ChAdOx1.HTI (C)) administered in a heterologous prime-boost regimen consisting of DDDMM and CCM versus placebo.

Participants had to be aged 18–65 years and have a history of triple-drug ART initiated within six months after estimated HIV-1 acquisition with an HIV-1 viral load of <50 HIV-1 RNA copies ml^{-1} and $CD4^+$ T cells >400 cells mm^{-3} for at least 12 and 6 months before inclusion, respectively. An in-house algorithm based on the Fiebig classification of HIV infection[15,37] and each participant's available HIV-1 diagnostic tests were used to calculate the estimated date of HIV-1 acquisition for each individual.

Before inclusion, all participants signed an informed consent previously reviewed by a local Community Advisory Board. The study was approved by the institutional ethical review board of HUGTIP (ref. no. AC-15-108-R) and by the Spanish Regulatory Authorities, and was conducted in accordance with the principles of the Helsinki Declaration and local personal data protection law (LOPD 15/1999).

For safety purposes, participants were randomized (2:1) into three sequential recruitment blocks after blinded safety reports were approved by an external SMC. A sentinel group of three participants (two vaccine recipients and one placebo recipient) was first enrolled, and one participant was randomized per day and monitored 24 h after each vaccination (group 1) to allow for the next sentinel participant to be vaccinated. The rest of the participants were part of the non-sentinel groups: group 2 ($n = 12$) and group 3 ($n = 30$). After completion of the first vaccination regimen (DDDMM/placebo), all 45 participants were offered to participate in a second phase of the study, which included a booster vaccination regimen with CCM or placebo (while maintaining the same treatment allocation from the initial regimen) and an ATI period of 24 weeks. Between DDDMM/placebo and CCM/placebo phases of the study, participants were kept on suppressive ART and performed clinical follow-ups every 12 weeks ('roll-over' period).

Criteria to proceed to ATI and resume ART

Eight weeks after the last vaccination (DDDMM-CCM or placebo) participants underwent an ATI of up to 24 weeks of duration if they had (1) received all vaccinations, (2) maintained a pVL of <50 copies ml^{-1} and $CD4^+$ T cells of >400 cells mm^{-3} and (3) there was no evidence of active syphilis, hepatitis B or hepatitis C infections. Before ATI start, HIV-seronegative participants' sexual partners were offered PrEP through a trial-specific PrEP-provision program. During the ATI, weekly visits were performed at HUGTIP, Badalona or at BCN-Checkpoint, Barcelona at participants' convenience. During the COVID-19 pandemic, remote visits and home-based blood draws were carried out. Criteria to resume ART included a single pVL of >100,000 copies ml^{-1}, pVL of >10,000 and ≤100,000 copies ml^{-1} for eight consecutive weeks, $CD4^+$ T cells <350 cells mm^{-3} in two consecutive determinations, development of a ≥grade 3 ARS, at the participant's request or investigator criteria. As part of investigator criteria, active surveillance for STIs was performed during the ATI and, if suggestive of unprotected sex with partners with unknown HIV status and/or HIV-negative partners not taking PrEP, ART was recommended to prevent HIV transmission. All participants off ART after 24 weeks of ATI were offered to resume ART except when pVL < 2,000 copies ml^{-1}. These participants were invited to participate in an ATI-extension protocol (NCT04385875). Criteria for ART resumption during the ATI-extension phase included one determination of pVL > 100,000 copies ml^{-1} or pVL > 2,000 copies ml^{-1} for eight consecutive weeks. Psychological assessments of the impact of the ATI on the emotional and sexual sphere were evaluated using trial-specific questionnaires by clinical psychologists at the HIV unit before entering the ATI, 12 weeks after the ATI, four weeks after ART was resumed and at the participants' request. Participants were followed 4 and 12 weeks after ART was resumed. The protocol and a list of amendments to the protocol are available as Supplementary files 1 and 2.

Study vaccines

The HTI immunogen is a chimeric protein sequence (total length of 529 amino acids (aa)) designed based on human immune reactivity[8] that includes 26 regions in HIV-1 Gag (45%), Pol (44%), Vif (8%) and Nef (3%) proteins identified in these analyses that (1) were preferentially targeted by participants with low viral loads and largely independent of beneficial HLA class I genotypes, (2) turned out to be more conserved than the rest of the proteome and (3) elicited responses of higher functional avidity and broader variant cross-reactivity than responses to other regions[9].

The DNA.HTI vaccine (D) is a circular and double-stranded DNA plasmid vector of 5,676 base pairs derived from the pCMVkan expression vector backbone expressing the codon-optimized HTI gene, preceded by the human granulocyte-macrophage colony-stimulating factor (GM-CSF) signal peptide for better secretion[12]. The DNA.HTI drug substance is manufactured, quality-control-tested and released in accordance with the requirements of good manufacturing practice (cGMP) by the Clinical Biotechnology Centre (CBC), Bristol Institute for Transfusion Sciences, University of Bristol, UK.

The MVA.HTI vaccine (M, modified Vaccinia virus Ankara) is a live, attenuated recombinant vaccinia (pox) virus attenuated by serial passages in cultured chicken-embryo fibroblasts that contains six large deletions from the parental virus genome[13]. The size of MVA.HTI after insertion of a transgene coding for the HTI insert is estimated to be ~179.6 kbp. Production was carried out by the German company IDT Biologika, and preparation, verification of the genetic stability and MSV and WSV storage were carried out at IDT under cGMP conditions and according to EU regulations.

The ChAdOx1.HTI vaccine (C)- is a replication-defective recombinant chimpanzee adenovirus (ChAd) vector based on a chimpanzee adenoviral isolate Y25[14] that encodes the HTI sequence. ChAdOx1.HTI was derived by subcloning the HTI antigen sequence into the generic ChAdOx1 BAC. The plasmid resulting from this subcloning (pC255; 40,483 bp) was linearized and transfected into commercial HEX293A T-REx cells to produce the vectored vaccine ChAdOx1.HTI. The ChAdOx1.HTI batch for non-clinical use was produced at the University of Oxford (UK), and large-scale amplification and purification of ChAdOx1.HTI were performed at ReiThera/Advent (Italy) according to cGMP.

Objectives

The primary objective of the study was to evaluate the safety and tolerability of HIV-1 vaccines DNA.HTI, MVA.HTI and ChAdOx1.HTI, administered intramuscularly as part of heterologous prime-boost regimen (DDDMM-CCM) in early-treated HIV-1-positive individuals. Secondary objectives included (1) evaluating the immunogenicity of DDDMM and CCM, (2) evaluating whether vaccination was able to prevent or delay viral rebound, induce post-rebound viral control and/or prevent or delay the need for resumption of ARV therapy during an ATI and (3) assessing the safety of the ATI period. Further immune (flow cytometry and viral inhibition assay) and viral evaluations (viral reservoir, autologous HIV-1 sequence and replicative fitness) were conducted as exploratory analyses. Post-hoc univariate and multivariate regression models were performed to explore potential correlates of virus control during ATI.

Safety

Safety was assessed by an analysis of local and systemic reactogenicity and laboratory data. All solicited local and systemic AEs were recorded during seven days after administration of each investigational medicinal product using a 'participant reactogenicity diary card'. Unsolicited AEs and SAEs were recorded at any point during the study. AEs were graded according to the Division of DAIDS table for grading the severity of adult and pediatric adverse events, version 2.1 (March 2017). Throughout the study, AEs were analyzed by period: from screening to ATI start and by DDDMM/CCM or placebo; during ATI and after ART resumption. The primary safety endpoint of the study was the proportion of participants who develop grade ≥3 AEs (including SAE) related to the investigational medicinal product (IMP) administration. AEs were specified as related or unrelated to the IMPs by the investigator. Per the *Manual for Expedited Reporting of Adverse Events to DAIDS* (version 2.0, January 2010), AEs were reported as related if there was reasonable possibility that the AE may be related to the study agent(s), as suggested by a plausible, reasonable time sequence existing in relation to administration of the drug, the observed manifestation coincided with the known adverse reactions profile of the implicated drug, and the event could not be or was unlikely to be explained by a concurrent disease or by other drugs or chemical substances. If there was not a reasonable possibility that the AE was related to the study agent(s), the AE was reported as unrelated.

SMC and risk-mitigation plan during the COVID-19 pandemic

An SMC formed by three external experts in pharmacovigilance and HIV vaccine trials plus four non-voting sponsor representatives reviewed all blinded safety data from the study at pre-specified timepoints (that is, before progressing recruitment groups and every three months thereafter). The SMC also reviewed and approved a risk-mitigation plan established to minimize the impact of the COVID-19 pandemic on the conduct of the trial. This plan included weekly ATI assessments with home-based blood draws by personnel protected with personal protective equipment and remote visits via phone; a taxi service for on-site visits; 24-h/7-d phone availability for reporting any COVID-19 symptoms; SARS-CoV-2 polymerase chain reaction (PCR) testing before any IMP dosing; and provision of ART by courier. The SMC met virtually every week from 16 March 2020 to 28 May 2020 to review all blinded safety and laboratory data, and decisions on whether to continue with the trial were based on the evolving situation of the local epidemic, site capacity and a case-by-case discussion. New ICF versions with emerging information on COVID-19 were also developed and reviewed by the institutional ethical review board of HUGTIP.

High-resolution HLA-A, -B and -C typing

The QIAsymphony DNA kit (Qiagen) was used for genomic DNA extraction. Genomic DNA was genotyped by screening for HLA class I molecules (HLA-A, HLA-B and HLA-C genes) at high resolution at the Histocompatibility and Immunogenetics Laboratory (www.bancsang.net). Briefly, three loci were genotyped simultaneously by an in-house multiplex long-range PCR (LRPCR). The library was prepared (enzymatic fragmentation, adapter ligation and barcoding) from the PCR pools using the NGSgo kit (GenDx) according to the manufacturer's instructions. The final denatured library was sequenced using a NextSeq or MiSeq sequencer (Illumina). HLA class I genotype determination was performed with NGSengine 2.9.1 software (GenDx) using the IMGT database as reference.

CCR5-Δ32 genotyping

DNA was extracted from cryopreserved PBMCs stored from roll-over phase timepoints from participants entering the ATI ($n = 41$). DNA samples were amplified using fluorescent PCR in a 9700 Gene Amp PCR System or 2720 Thermal Cycler (Applied Biosystems) as described in ref. [38]. The forward (TTCATTACACCTGCAGCTCTC) and reverse (FAM-CCTGTTAGAGCTACTGCAATTAT) primers produced a 270-bp product for the CCR5-Δ32 allele and a 302-bp PCR product for the CCR5-WT allele. After amplification, 0.5 µl of PCR products was mixed in a 1:10 dilution with 24 µl of Hi-Di formamide (Applied Biosystems) and 0.7 µl of Gene Scan-500 ROX Size Standard (Applied Biosystems) and denatured at 94 °C for 5 min. The capillary electrophoresis was carried out in a 3130xlGenetic Analyzer (Applied Biosystems) and samples were analyzed with GeneMapper software (Applied Biosystems).

Sequencing

Whole-genome deep sequencing of the HIV-1 genome, including *gag*, *pol*, *vif* and *nef* genes, was performed using the Illumina NexteraXT protocol and a MiSeq platform with 300-bp paired-end sequencing length. Raw sequencing data were analyzed wih PASeq v 1.14 (www.paseq.org[39]). In brief, quality filter and adapter trimming was performed using trimmomatic[40]. High-quality sequences were aligned against the HXB2R reference using Bowtie2[41]. The consensus sequence at 20% frequency threshold was called using samtools[42] and a multiple alignment including all sequences was generated using MAFFT[43]. For each sample-specific consensus nucleotide sequence, subtyping was performed using the COMET online tool[44], and the Tamura–Nei nucleotide and Jones–Taylor–Thornton (JTT) amino-acid distances versus HXB2R and HTI sequences, respectively, were calculated using the R::phangorn package[45]. The number of mismatches (hamming) versus the HTI sequence was also calculated for all segments and aggregated at the protein level. The percentage difference (%AA.mm versus HTI) was calculated over the total length of the segment, correcting for the uncovered position in each sample. Group comparisons were performed using the Mann–Whitney *t*-test.

IFN-γ-ELISpot assay

Total HTI and HIV-1-specific T cells were assessed ex vivo using freshly isolated PBMCs with an IFN-γ-detecting enzyme-linked immunoabsorbent spot assay (ELISpot IFN-γ Mabtech kit) as previously described[2]. 15-mer peptides overlapping by 11 amino acids were combined into ten pools spanning different HIV-1 proteins/subproteins of 7–22 peptides per pool corresponding to the HTI vaccine insert (P1–P10, total $n = 111$ peptides, Thermo Fisher) and eight pools of 62–105 peptides per pool spanning the rest of the HIV-1 viral protein sequences (OUT P1–P8, total $n = 637$ peptides, obtained through the NIH AIDS Reagent Program). All peptide pools used in fresh ELISpots were tested in duplicate with a final concentration of individual peptide of 1.55 µg ml^{-1}. Medium only was used as no-peptide negative control in quadruplicate wells. Positive controls included two peptide pools covering lytic ($n = 16$) and latent ($n = 36$) Epstein–Barr viral proteins (1.55 µg ml^{-1}, Thermo Fisher), phytohaemagglutinin (PHA; 50 µg ml^{-1}, Sigma) and a chicken-embryo-fibroblast peptide pool (2 µg ml^{-1}) consisting of 32 previously defined human CD8$^+$ T-cell epitopes from cytomegalovirus, Epstein–Barr virus and influenza virus (Pantec). Spots were counted using an automated Cellular Technology Limited (C.T.L.) ELISpot reader unit. The threshold for positive responses was set at ≥50 SFCs per 10^6 PBMCs (five spots per well), greater than the mean number of SFCs in negative control wells plus three standard deviations of the negative control wells, or more than three times the mean of negative control wells, whichever was higher.

Mapping of HTI-specific responses

IFN-γ ELISpot assays using 147 individual overlapping peptides covering the entire HTI sequence were performed in in vitro expanded T cells. Participants' cryopreserved PBMCs obtained at baseline (week 0) and after DDDMM (week 24) and CCM or placebo vaccinations (week 28) were expanded using an anti-CD3 mAb (12F6) and kept in culture until sufficient cell numbers were reached for each timepoint[46]. Two consecutive overlapping peptides were considered one individual HTI response, and the highest magnitude of the sequential responses

was taken as the magnitude for each identified response. The results were expressed as the number of positive responses to individual peptides as well as the distribution among the different HIV subprotein regions covered by HTI: Vif-Nef, Pol-Int, Pol-RT, Pol-Prot, Gag-p2p7p1p7, Gag-p24 and Gag p17.

Intracellular cytokine staining assay

Cryopreserved PBMCs from week 28 (four weeks after completion of the last series of vaccinations, DDDMM-CCM) were used for stimulation with four pools of 9–43 peptides per pool spanning p17, p24/p15, Pol and Vif/Nef regions included in the HTI vaccine insert. Peptides were added at a final concentration of 5 μg ml^{-1} of each peptide in the presence of both 1.4 μg ml^{-1} of anti-CD28 (BD Bioscience) and 1.4 μg ml^{-1} anti-CD49d (BD Bioscience). As positive controls for the assay, cells were cultured alone in the presence of (1) anti-CD3/28 Dynabeads (Thermo Fisher Scientific) according to the manufacturer's instructions or (2) 10 ng ml^{-1} phorbol 12-myristate 13-acetate (PMA,Sigma) and 1 μM ionomycin (Sigma). Cells stimulated with only anti-CD28 and anti-CD49d antibodies or with DMSO were used as negative controls. Stimulated cells were incubated for 6 h at 37 °C in 5% CO_2, in the presence of 4 μl of monensin (GolgiStop, BD Bioscience). After 6 h of stimulation, cells were incubated with a Live/Dead fixable Violet Dead cell stain kit (Invitrogen), for exclusion of dead cells, along with the exclusion of monocytes and B cells by including in the dump channel anti-CD14 and anti-CD19 antibodies. Surface markers of T-cell lineage (CD3, CD4 and CD8), follicular T cells (CXCR5 and PD1), T-cell phenotype (CD45RA and CCR7), T-cell activation (CD69 and HLADR) and T-cell exhaustion (TIGIT, PD1) were included as well. Cells were fixed and permeabilized using the Cell Fixation and Cell Permeabilization Kit (Invitrogen) and intracellularly stained for INF-γ, GrazymeB, IL-2 and TNF-α. Details on the used antibodies can be found in the Reporting summary. Cells were resuspended in phosphate buffered saline supplemented with 1% FBS and acquired on an LSR Fortessa flow cytometer (BD, Unidad de Citometria, IGTP) and analyzed using FlowJo. The gating strategy is shown in Supplementary Fig. 2. When needed for variably expressed antigens, fluorescence minus one was included to define the boundaries between positive and negative populations. At least 100,000 total events were recorded. The frequencies of cells that produce all possible combinations of intracellular cytokines were calculated using the Boolean gating function of the FlowJo software. Data were reported after background subtraction (from the unstimulated negative control), and HTI-specific responses were defined as the sum of the specific population for each of the four HTI peptide pool stimulations.

In vitro viral suppressive capacity (VIA assay)

$CD8^+$ T-cell-mediated viral inhibition capacity was measured at 1:1 and 1:10 CD8-effector to CD4-target ratios, as previously described[47,48]. Autologous $CD4^+$ cells were obtained as targets from samples before vaccination where $CD8^+$ cells were depleted by magnetic bead separation (MACS Milteny Biotec). $CD8^+$-depleted cells ($CD4^+$-enriched fraction) were stimulated with PHA for three days and then infected by spinoculation with HIV-1 BAL and IIIB laboratory-adapted strains and autologous HIV-1 viruses at a multiplicity of infection of 0.001. HIV-infected cells were cultured in triplicates in R10 medium with 20 U ml^{-1} of IL-2 in 96-well round-bottomed plates, alone or together with effector $CD8^+$ T cells obtained by positive magnetic bead separation the same day from an additional vial of cryopreserved PBMCs from baseline and after DDDMM (week 24) and CCM or placebo (week 28) vaccinations. Viral replication was measured as the production of HIV-1 antigen p24 in culture supernatants (pg p24 per ml) at day 5 of co-culture using an Innogenetics p24 Elisa kit, and inhibition was expressed as a percentage with respect to the positive control of each virus (that is, infection in the absence of $CD8^+$ T cells).

Total and intact proviral HIV-1 DNA

To distinguish deleted and/or hypermutated proviruses from intact proviruses, total and intact proviral (IPDA) HIV-1 DNA copies in $CD4^+$ T cells were measured at screening and ATI start in extracts of lyzed $CD4^+$ T cells by digital droplet PCR (ddPCR), as previously described[49]. Samples from 41 participants that entered into the ATI period were processed at Accelevir Diagnostics. The DNA shearing index was calculated, and values for intact and defective proviruses were normalized to copies per 10^6 input cells (determined by RPP30, the gene encoding Ribonuclease P protein subunit p30) and adjusted for shearing using the DNA shearing index. Results were expressed as HIV-1 DNA copies (counts) per 10^6 $CD4^+$ T cells.

Viral fitness of participants' autologous HIV-1 viruses

The viral replication capacity of autologous HIV-1 viruses was measured for 38 of the 41 participants that entered into the ATI period. For isolation of autologous HIV-1 viruses, the CD4-enriched fraction of cryopreserved PBMCs stored at HIV-1 diagnosis pre/or within the first weeks of ART initiation were thawed and co-cultured with CD8-depleted PBMCs previously activated from three different healthy donors until HIV-1 was collected from supernatants. To determine the viral replication kinetics, a pool of PBMCs from three healthy donors, previously stimulated with 20 U ml^{-1} of IL-2 and PHA for three days, were infected by spinoculation at a multiplicity of infection of 0.001. HIV-1 antigen p24 was measured in culture supernatants (pg p24 per ml) using a commercial ELISA kit from Innogenetics at days 0, 3, 4, 5, 6 and 7 post-infection, and replication capacity was calculated by fitting a linear model to the log-transformed p24 data during the exponential growth phase. Uninfected cells and those infected with laboratory-adapted CCR5- and CXCR4-tropic viruses ($HIV\text{-}1_{NL43}$, $HIV\text{-}1_{BaL}$ and $HIV\text{-}1_{IIIB}$ isolates isolates) in the presence and absence of the antiretroviral AZT were used as reference values or controls.

Statistics

There was no power calculation for this study. The sample size was proposed to provide preliminary safety information on the vaccine regimen (primary objective). As a means to characterize the statistical properties of this study for the safety primary endpoint, in terms of the chances of observing an AE, 30 participants in the active group provided a high probability (78.5%) that this study would observe at least one event if the event occurred in the population with a true rate of 5%.

Time to viral load detection was calculated from the ATI start date to the date of first occurrence of pVL of ≥50 copies ml^{-1} and time off ART was calculated from the ATI start date to the date of ART resumption. Participants who prematurely resumed ART for COVID-19-related reasons were not censored for the survival analysis. The time to event was derived using the number of days between the ATI start date and the date of event expressed in weeks (number of days/7). The Kaplan–Meier estimator was used to describe the time to ART resumption, and survival functions were compared using the log-rank test. Differences in medians between groups were compared using the Mann–Whitney test and Fisher test, when corresponding. Spearman's ρ was used for correlations. All tests were two-sided, unadjusted for multiple comparisons, with 5% error rate. Post-hoc univariate logistic regression models (the list of considered covariates is provided in Extended Data Table 5) were considered to select the covariates with $P < 0.25$ to be included in the multivariate models. All selected covariates were analyzed for possible multicollinearity. Considering the final selected covariates, multivariate logistic regression models were adjusted for the binary outcome of time off ART ≥ 12 weeks versus <12 weeks. Analyses were performed using R project 3.6.2 (https://www.r-project.org/) and GraphPad Prism version 9.1.2 for Windows (GraphPad Software, https://www.graphpad.com). Flow cytometry data were preprocessed using FlowJo software version 10.6 and imported into Pestle2/SPICE software v5.35 (Vaccine Research Center, NIAID/NIH) for graphical representation.

Polyfunctional bar plots per treatment group were compared using the Mann–Whitney test per row, with individual ranks computed for each comparison. The two-stage linear step-up procedure of Benjamini, Krieger and Yekutieli was used to control for false discovery rate. All performed analyses matched the pre-specified statistical analysis plan (AELIX002-SAP, version 2, from 10 July 2020).

Reporting summary

Further information on research design is available in the Nature Research Reporting Summary linked to this Article.

Data availability

Deep sequencing raw data obtained from sequencing have been deposited in GenBank (accession no. PRJNA751460). Requests for access to the study data can be submitted through the Yale Open Data Access (YODA) Project site at http://yoda.yale.edu.

References

38. Enrich, E. et al. Analysis of the Spanish CCR5-Δ32 inventory of cord blood units: lower cell counts in homozygous donors. *Bone Marrow Transpl.* **53**, 741–748 (2018).
39. Noguera-Julian, M. et al. Next-generation human immunodeficiency virus sequencing for patient management and drug resistance surveillance. *J. Infect. Dis.* **216**, S829–S833 (2017).
40. Bolger, A. M., Lohse, M. & Usadel, B. Trimmomatic: a flexible trimmer for Illumina sequence data. *Bioinformatics* **30**, 2114–2120 (2014).
41. Langmead, B. & Salzberg, S. L. Fast gapped-read alignment with Bowtie 2. *Nat. Methods* **9**, 357–359 (2012).
42. Li, H. et al. The Sequence Alignment/Map format and SAMtools. *Bioinformatics* **25**, 2078–2079 (2009).
43. Katoh, K. & Standley, D. M. MAFFT multiple sequence alignment software version 7: improvements in performance and usability. *Mol. Biol. Evol.* **30**, 772–780 (2013).
44. Pineda-Peña, A. C. et al. Automated subtyping of HIV-1 genetic sequences for clinical and surveillance purposes: performance evaluation of the new REGA version 3 and seven other tools. *Infect. Genet. Evol.* **19**, 337–348 (2013).
45. Schliep, K. P. phangorn: phylogenetic analysis in R. *Bioinformatics* **27**, 592–593 (2011).
46. Kawana-Tachikawa, A. et al. Effect of maraviroc intensification on HIV-1-specific T cell immunity in recently HIV-1-infected individuals. *PLoS ONE* **9**, e87334 (2014).
47. Yang, H. et al. Antiviral inhibitory capacity of $CD8^+$ T cells predicts the rate of $CD4^+$ T-cell decline in HIV-1 infection. *J. Infect. Dis* **206**, 552–561 (2012).
48. Ross-Umbert, M. In vivo effects of romidepsin on T-cell activation, apoptosis and function in the BCN02 HIV-1 Kick&Kill Clinical Trial. *Front. Immunol* **11**, 418 (2020).
49. Bruner, K. M. et al. A quantitative approach for measuring the reservoir of latent HIV-1 proviruses. *Nature* **566**, 120–125 (2019).

Acknowledgements

Special thanks go to all the volunteers participating in this study for their perseverance and dedication. We especially thank the SMC members E. Negredo, M. Farré and F. Garcia for their commitment to oversee the risk-mitigation plan during the challenging COVID-19 pandemic. We thank R. Ayen, L. Gómez, C. Ramírez and E. Grau from the sample processing laboratory at IrsiCaixa, Badalona, Spain for their technical assistance throughout the study. We thank B. K. Felber and G. N. Pavlakis from the NCI-Frederick, MD, USA and A. Crook from the Jenner Institute, The Nuffield Department of Medicine, University of Oxford, UK for their assistance in the construction and provision of the pre-GMP starting materials of DNA.HTI, MVA.HTI and ChAdOx1.HTI under MTA contracts. This work was supported by AELIX Therapeutics SL, and partly by grants from the Spanish Research Agency and the European Regional Development Fund under contract no. RTC-2017-6473-1 ((AEI/FEDER, UE)/(MINECO/FEDER, UE)), the European Union's Horizon 2020 research and innovation program under grant agreement 681137-EAVI2020, NIH grant P01-AI131568 and by ISCIII PI20/01039. L.B. held a PhD grant from ISCIII (RH CM20/00097) during the conduct of the study. This study was funded by AELIX Therapeutics SL, who participated in the design of the study, provided the IMP of the study, oversaw all safety monitoring activities, data analysis and interpretation, and reviewed the manuscript.

Author contributions

C.B., I.M., J.M. and B.M. conceived and designed the study. L.B. and A.L. additionally contributed to the study design in further study amendments. L.B., J.C., C.L., M.L., J.M., B.M., F.P. and A.R. contributed with clinical development of the study. A.L., M.L., B.O.-T., F.P., F.P.E. and D.S. contributed to data management and overall study coordination. T.H. and E.G.W. helped with IMP production. M.C., S.C., T.E., A.L.L., M.P. and M.R.-U. performed the experiments. Y.A.-S., A.L.L., J.M., B.M., M.R.-R. and M.N.-J. undertook the statistical analysis. L.B., C.B., J.M. and B.M. drafted the manuscript. L.B., A.L., I.M., D.S., B.C., C.B., J.M., B.M. and R.P. critically revised the manuscript for important intellectual content. All authors reviewed and approved the final version of the manuscript.

Competing interests

C.B., B.M. and A.L.L. are co-inventors of the HTI immunogen (patent application PCT/EP2013/051596). C.B., B.M. and I.M. are co-inventors of US patent application no. 62/935,519 and US patent application no. 62/851,546, which have relevance to the vaccine regimen used in this study. B.M. reports consultancy personal fees from AELIX Therapeutics SL, as well as speakers' fees from Gilead, Janssen and ViiV Healthcare, outside the submitted work. C.B. is co-founder, CSO and shareholder of AELIX Therapeutics SL and serves as an advisor for Tendel Therapies and OmniScope, outside the submitted work. M.N.-J. is co-founder and shareholder of Nano1Health SL, outside the scope of the submitted work. I.M. is a shareholder of, and acts as a consultant to, AELIX Therapeutics SL. He is also the CMO of Orion Biotechnology, outside the scope of the submitted work. J.M. has received research funding, consultancy fees and lecture sponsorships from, and has served on advisory boards for, various laboratories (MSD, Abbvie, Boehringer Ingelheim, Gilead Sciences, Viiv Healthcare, Janssen-Cilag and Bristol-Myers-Squibb). The remaining authors declare no competing interests.

Additional information

Extended data is available for this paper at https://doi.org/10.1038/s41591-022-02060-2.

Supplementary information The online version contains supplementary material available at https://doi.org/10.1038/s41591-022-02060-2.

Correspondence and requests for materials should be addressed to Jose Molto.

Peer review information *Nature Medicine* thanks Zaza Ndhlovu, Cecilia Moore and the other, anonymous, reviewer(s) for their contribution to the peer review of this work. Primary Handling Editor: Alison Farrell, in collaboration with the *Nature Medicine* team.

Reprints and permissions information is available at www.nature.com/reprints.

https://doi.org/10.1038/s41591-022-02060-2

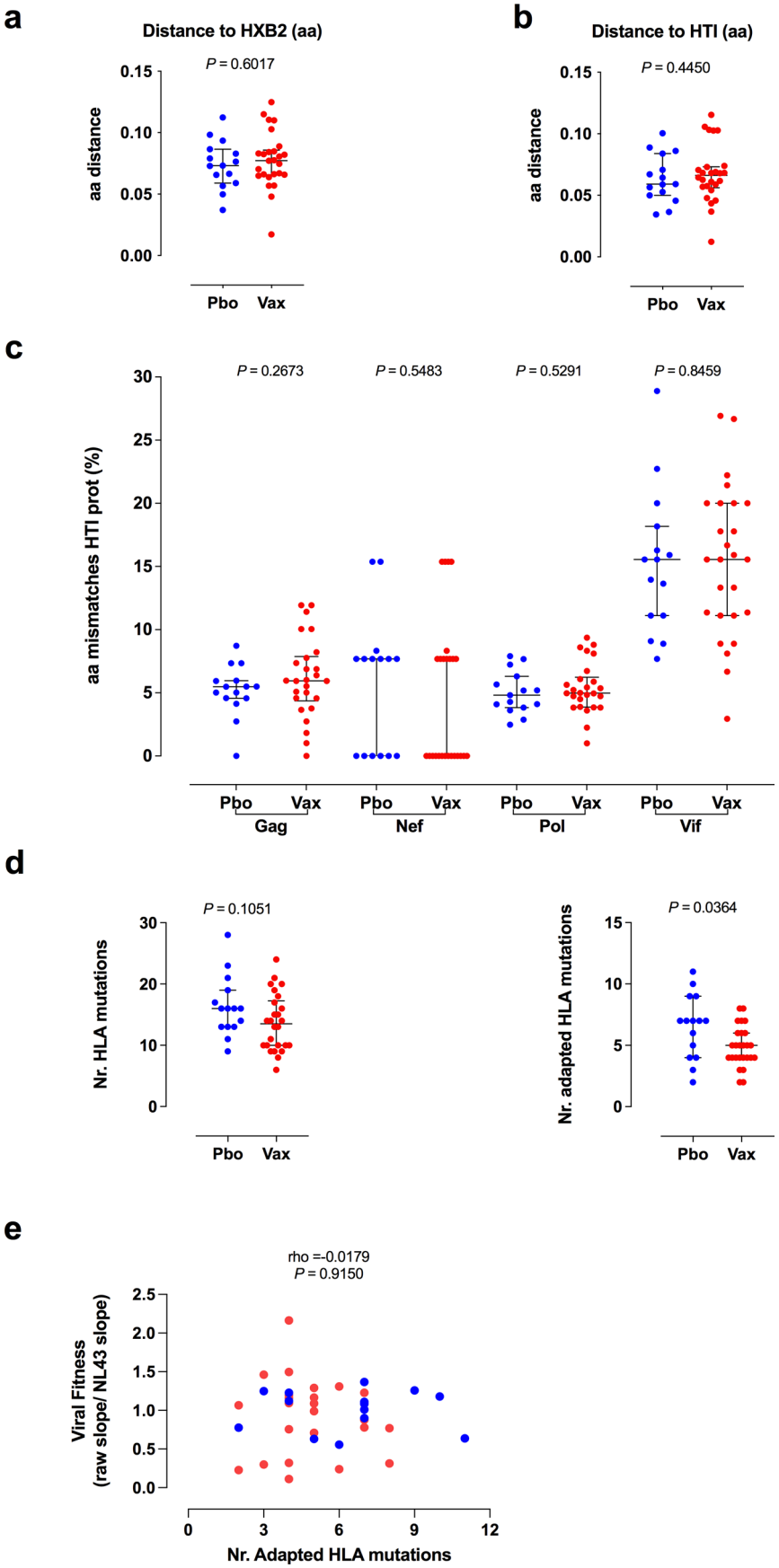

Extended Data Fig. 1 | See next page for caption.

https://doi.org/10.1038/s41591-022-02060-2

Extended Data Fig. 1 | Pre-ART HIV-1 sequences. Coverage of the participant's HIV-1 sequences by HTI vaccine. Comparison of distance with HXB2 (Tamura-Nei) in (a) and HTI (JTT) (b) for placebo (n=15, blue) and vaccine (n=26, red) recipients. *Mann-Whitney t-test is shown*. c, Genetic distance between the placebo (blue) and vaccine (red) recipient's pre-ART HIV-1 sequences and different HIV-1 proteins included in the HTI immunogen. *Mann-Whitney t-test is shown* d, Number of total HLA (left) and HLA-adapted (right) polymorphisms on pre-ART HIV-1 sequences from placebo (n=15, blue) and vaccine (n=26, red) recipients. *Mann-Whitney t-test is shown*. For (a)-(d), median with interquartile range is shown. e, Correlation between the number of pre-ART CTL escape footprints and replicative fitness of autologous pre-ART HIV-1 sequences from placebo (n=14, blue) and vaccine (n=24, red) recipients. *Spearman's correlation is used. Pbo:* placebo, *Vax:* vaccine.

https://doi.org/10.1038/s41591-022-02060-2

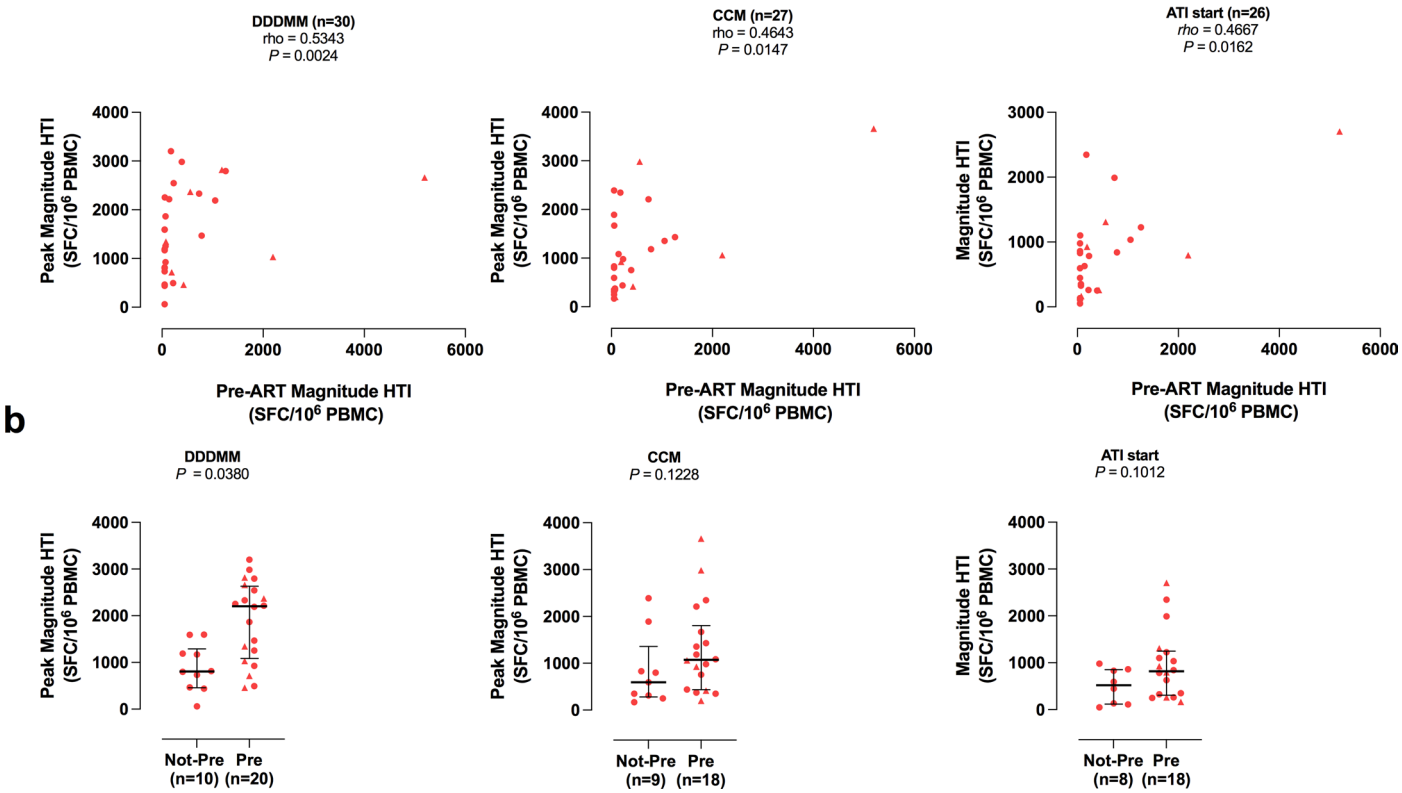

Extended Data Fig. 2 | Role of pre-existing responses to HTI. a, Relation between pre-ART HTI-specific responses and expanded HTI responses at peak immunogenicity timepoints after DDDMM, CCM and ATI start in all vaccine recipients are shown and individuals with any beneficial HLA allele are represented in triangle. *Spearman's correlation is used*. b, Peak HTI- magnitude after DDDMM (n=30), CCM (n=27) and at ATI start (n=26) for all the vaccine recipients having or not having any HTI responses before any ART (*Pre*, defined as HTI magnitude >50 SFC/10^6 PBMC). Individuals with a beneficial HLA are shown in triangle symbols. Median with interquartile range is shown. Wilcoxon-Mann-Whitney test was used for comparison between treatments. *C:* ChAdOx1.HTI, *D:* DNA.HTI, *M:* MVA.HTI, *P:* placebo, *ART:* antiretroviral treatment, *ATI:* analytical treatment interruption.

https://doi.org/10.1038/s41591-022-02060-2

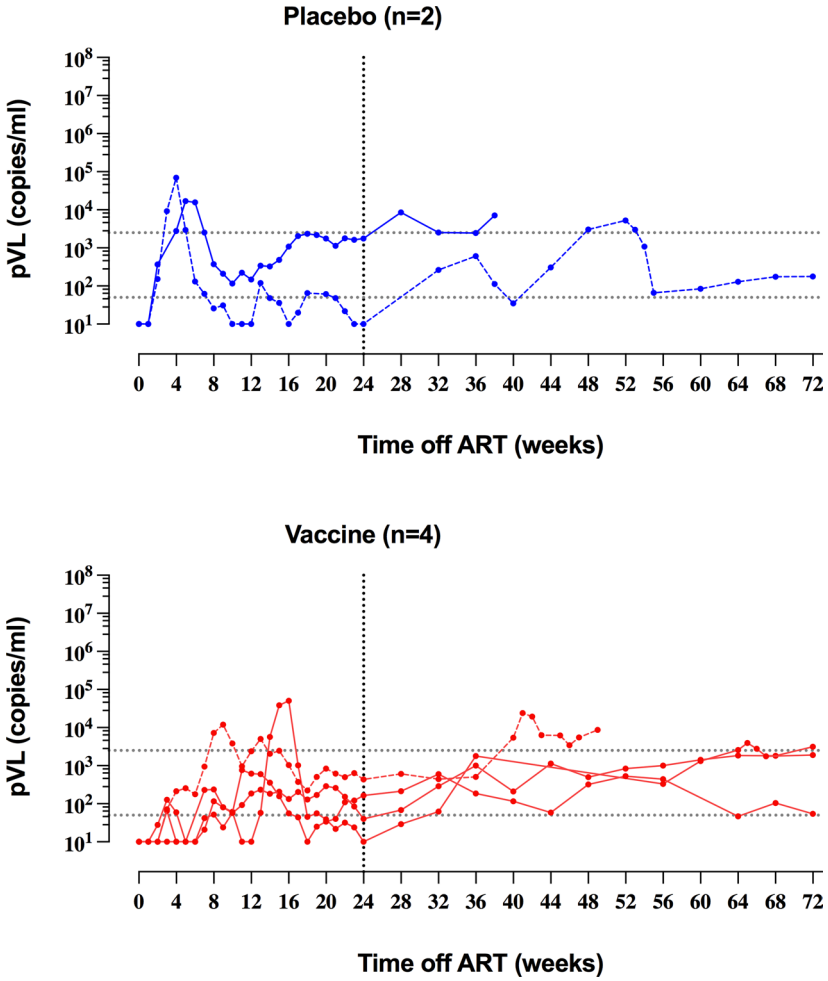

Extended Data Fig. 3 | ATI-extension beyond 24 weeks. Extended individual pVL up to 72 weeks is shown for placebo (blue) or vaccine (red) recipients that entered into the ATI-extension protocol (>24 weeks). Lines are interrupted on day of ART resumption, that is at week 72 or before. Dotted lines represent individuals with beneficial HLA class I alleles. *ATI:* analytical treatment interruption, *pVL:* plasma viral load.

https://doi.org/10.1038/s41591-022-02060-2

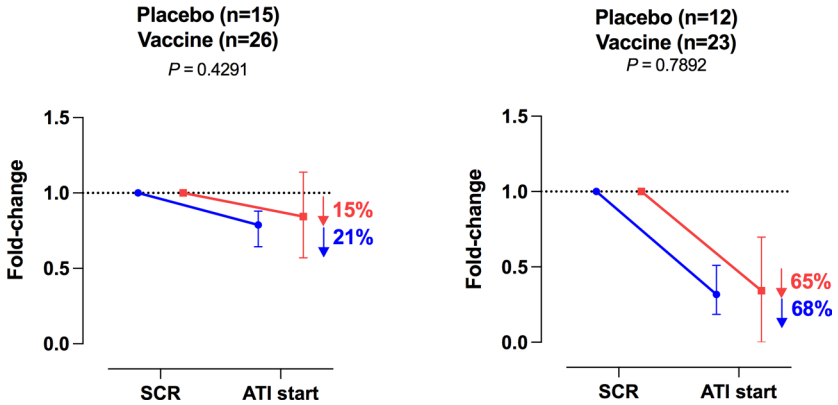

Extended Data Fig. 4 | HIV-1 reservoir decay throughout the study. Fold-change decay for total (placebo n=15, vaccine n=26) and intact (placebo n=12, vaccine n=23) proviral HIV-1 DNA by treatment group from study entry to ATI start. Median and interquartile range are represented. Mann-Whitney test is used. *SCR*: screening, *ATI*: analytical treatment interruption.

https://doi.org/10.1038/s41591-022-02060-2

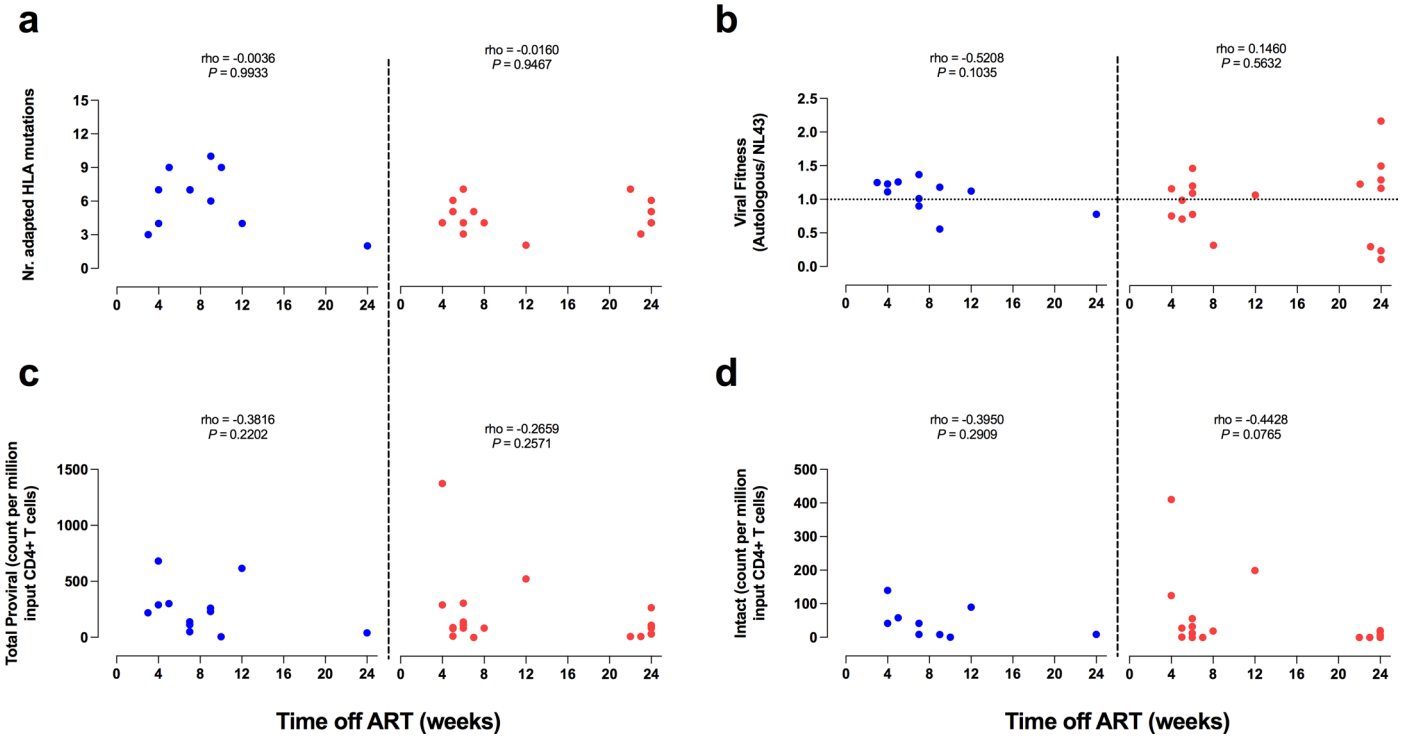

Extended Data Fig. 5 | Virological correlates with ATI outcomes in participants without any beneficial HLA allele. a, Correlation between number of HLA-adapted polymorphisms in pre-ART HIV-1 sequences and time off ART in placebo (blue) and vaccine (red) recipients. b, Correlation between replication capacity of participant's autologous HIV-1 virus (relative to NL43) replication and time off ART in placebo (blue) and vaccine (red) recipients. Correlation between levels of total (c) and intact (d) proviral HIV-1 DNA at ATI and time off ART in placebo (blue) and vaccine (red) recipients. *Spearman's correlation is used. ART:* antiretroviral treatment, *ATI:* analytical treatment interruption.

https://doi.org/10.1038/s41591-022-02060-2

Extended Data Table 1 | Summary overview of all adverse events during the study

	Placebo		Vaccine		Total	
	Episodes n	Participants n (%)	Episodes n	Participants n (%)	Episodes n	Participants (%)
AE information						
Total AEs	238	15 (100)	570	30 (100)	808	45 (100)
Local AEs	12	6 (40)	108	29 (96.7)	120	35 (77.8)
Systemic AEs	226	15 (100)	462	29 (96.7)	688	44 (97.8)
Treatment-related AEs	111	15 (100)	329	30 (100)	440	45 (100)
SAEs related	0	0 (0)	0	0 (0)	0	0 (0)
SAEs	0	0 (0)	2	2 (6.67)	2	2 (4.4)
AEs leading to withdrawal	0	0 (0)	0	0 (0)	0	0 (0)
Deaths	0	0 (0)	0	0 (0)	0	0 (0)
Intensity of AEs						
Grade 1	142	15 (100)	351	30 (100)	493	45 (100)
Grade 2	94	15 (100)	210	29 (96.7)	304	44 (97.8)
Grade 3	2	2 (13.3)	8	6 (20)	10	8 (17.8)
Grade 4	0	0 (0)	1	1 (3.3)	1	1 (2.2)
Study Period						
DDDMM/PPPPP regimen	76	15 (100)	229	29 (96.7)	305	44 (97.8)
CCM/PPP regimen	35	11 (73.3)	100	22 (81.5)	135	33 (78.6)
ATI	22	11 (73.3)	42	18 (69.2)	64	29 (70.7)
Post-ATI	10	4 (30.8)	11	9 (40.9)	21	13 (37.1)

AE, adverse event; SAE, serious adverse event; C, ChAdOx1.MTI; D, DNA.HTI; M, MVA.HTI; P, placebo; ATI, Analytical Treatment Interruption.

https://doi.org/10.1038/s41591-022-02060-2

Extended Data Table 2 | Primary endpoint: All Grade 3 or 4 adverse events from baseline to ATI start (sorted by group of treatment)

PT	Group	Grade	Latest vaccination	Outcome	Related	SAE
Epididymitis	Placebo	3	Pbo2	Resolved	No	No
Hypertriglyceridaemia	Placebo	3	-	Resolved	No	No
Appendicitis	Vaccine	4	-	Resolved	No	Yes‡
Depression	Vaccine	3	-	Ongoing	No	No
Vertigo	Vaccine	3	-	Resolved	No	No
Asthenia/Fatigue	Vaccine	3	MVA3	Resolved	Yes	No
Gastroenteritis	Vaccine	3	-	Resolved	No	Yes‡
Gastroenteritis	Vaccine	3	-	Resolved	No	No
Musculoesletetal chest pain	Vaccine	3	-	Resolved	No	No
Myalgia	Vaccine	3	-	Resolved	No	No
Neck pain	Vaccine	3	DNA1	Resolved	No	No

‡ Required inpatient hospitalization.

ATI, Analytical Treatment Interruption; SAE, serious adverse event; Pbo2, 2nd placebo administration; MVA3, 3rd MVA.HTI vaccination; DNA1, 1st DNA.HTI vaccination.

https://doi.org/10.1038/s41591-022-02060-2

Extended Data Table 3 | Secondary Endpoint: Increases in HTI magnitude at peak immunogenicity timepoint

Parameter	Placebo (n=15)	Vaccine (n=30)	*p-value*[a]
Immune parameter			
HTI-magnitude	185 (50 to 1,080)	1,593 (170 to 3,660)	*0.0000*
HTI-magnitude change	100 (0 to 498)	1,499 (120 to 3,150)	*0.0000*
Percentage of Responders			
2-fold increase from BSL, n (%)	10 (66.7)	29 (96.7)	*0.0117*
3-fold increase from BSL, n (%)	2 (13.3)	29 (96.7)	*0.0000*
Specific 3-fold increase from BSL, n (%)[b]	1 (7)	24 (80.0)	*0.0000*

[a] *Wilcoxon-Mann-Whitney test or Fisher Exact test for comparison between treatment arms when appropriate.*

[b] *At peak immunogenicity timepoint, increase in HTI magnitude >3-fold from baseline value provided that responses to non-HTI regions are <3-fold from their baseline value*

https://doi.org/10.1038/s41591-022-02060-2

Extended Data Table 4 | Secondary Endpoint. Parameters of interest during the ATI

Clinical parameter	Placebo (n=15)	Vaccine (n=26)	p-value
Time to first pVL >50 copies/ml (weeks)	2 (1 -6)	3 (1 – 9)	0.1942
pVL (copies/ml) at first positive determination	553 (59 – 14,632)	214 (52 – 17,180)	0.2314
Time to pVL > 10,000 (weeks)	4 (1 – 19)**	5 (2 – 24$^{\mp}$)**	0.1085*
Time to pVL peak (weeks)	5 (3 – 24)	6 (3 – 24)	0.2232
pVL (copies/ml) at peak determination	114,660 (16,868 – 980,171)	212,057 (289 - 10,000,000)	0.9460
Slope (log10(copies)/ml·weeks)	1.07 (0.07 – 1.69)	1.07 (0.04 – 2.18)	0.6847
Last pVL at end of ATI (copies/ml)	63,090 (10– 980,171)	64,866 (10 – 10,000,000)	0.5697
AUC normalized by weeks (log10(copies)/ml)	3.26 (1.80 - 4.30)	3.22 (1.68 – 3.91)	0.4648
Time off ART (weeks)	9 (3 – 24$^{\mp}$)**	7.5 (4 - 24$^{\mp}$)**	0.5755*
CD4 cell count at ATI start	865 (467 -1,502)	820 (470 – 1,462)	0.5882
CD4 cell count at end of ATI	687 (413 – 1,125)	645 (380 – 1,303)	0.4985

$^{\mp}$ Censored at this time point, did not reach the event within 24 weeks of ATI (>24).
** Log-rank test used.*
*** Median survival time, minimum and maximum time presented.*
pVL <20 or <40 cop/ml (UD) is computed as 10 copies/ml & pVL >10,000,000 cop/ml is computed as 10,000,000 copies/ml.
pVL, plasma viral load; ATI, analytical treatment interruption; AUC, area under the curve.

https://doi.org/10.1038/s41591-022-02060-2

Extended Data Table 5 | Multivariate logistic regression model for resuming ART >12 weeks considering covariates at AELIX-002 entry (n=32 participants without beneficial alleles)

	$\widehat{\beta}$	$s.e.(\widehat{\beta})$	$\widehat{OR}$	95% CI ($\widehat{OR}$)
(Intercept)	2.9567	3.2682		
Treatment (Vax)	2.1105	1.1929	8.25	1.05 ; 140.36
pVL at ART initiation (1 log10 copies/mL)	-1.5881	0.7807	0.20	0.03 ; 0.73
Ratio CD4/CD8 at AELIX-002 entry (0.2 units)	0.4070	0.8943	1.50	1.10 ; 65.77

Vax, vaccine; pVL, plasma viral load; ART, antiretroviral treatment.

nature portfolio

Corresponding author(s): jmolto@lluita.org

Last updated by author(s): Sep 27, 2022

Reporting Summary

Nature Portfolio wishes to improve the reproducibility of the work that we publish. This form provides structure for consistency and transparency in reporting. For further information on Nature Portfolio policies, see our Editorial Policies and the Editorial Policy Checklist.

Statistics

For all statistical analyses, confirm that the following items are present in the figure legend, table legend, main text, or Methods section.

n/a	Confirmed
☐	☒ The exact sample size (*n*) for each experimental group/condition, given as a discrete number and unit of measurement
☐	☒ A statement on whether measurements were taken from distinct samples or whether the same sample was measured repeatedly
☐	☒ The statistical test(s) used AND whether they are one- or two-sided *Only common tests should be described solely by name; describe more complex techniques in the Methods section.*
☐	☒ A description of all covariates tested
☐	☒ A description of any assumptions or corrections, such as tests of normality and adjustment for multiple comparisons
☐	☒ A full description of the statistical parameters including central tendency (e.g. means) or other basic estimates (e.g. regression coefficient) AND variation (e.g. standard deviation) or associated estimates of uncertainty (e.g. confidence intervals)
☐	☒ For null hypothesis testing, the test statistic (e.g. *F*, *t*, *r*) with confidence intervals, effect sizes, degrees of freedom and *P* value noted *Give P values as exact values whenever suitable.*
☒	☐ For Bayesian analysis, information on the choice of priors and Markov chain Monte Carlo settings
☒	☐ For hierarchical and complex designs, identification of the appropriate level for tests and full reporting of outcomes
☐	☒ Estimates of effect sizes (e.g. Cohen's *d*, Pearson's *r*), indicating how they were calculated

Our web collection on statistics for biologists contains articles on many of the points above.

Software and code

Policy information about availability of computer code

Data collection	Clinical data was collected thourgh an eCRD designed by Dynasolutions.
Data analysis	Statistical analyses were performed using R version 3.6.2 (2019 The R Foundation for Statistical Computing, https://www.r-project.org/) and GraphPad Prism version 9.1.2 (226) for Windows (https://www.graphpad.com). Preprocessing of flow cytometry data was performed using both FlowJo software version 10.6 and imported into Pestle2/ SPICE software v5.35 (Vaccine Research Center, NIAID/NIH, Bethesda, MD, USA) for graphical representation

For manuscripts utilizing custom algorithms or software that are central to the research but not yet described in published literature, software must be made available to editors and reviewers. We strongly encourage code deposition in a community repository (e.g. GitHub). See the Nature Portfolio guidelines for submitting code & software for further information.

Data

Policy information about availability of data

All manuscripts must include a data availability statement. This statement should provide the following information, where applicable:

- Accession codes, unique identifiers, or web links for publicly available datasets
- A description of any restrictions on data availability
- For clinical datasets or third party data, please ensure that the statement adheres to our policy

Deep sequencing raw data obtained from sequencing have been deposited in GenBank (accesion PRJNA751460). Requests for access to the study data can be

submitted through the Yale Open Data Access (YODA) Project site at http://yoda.yale.edu. Full answers to the journal´s questions about data access can be found on the Yoda website but briefly, there is a review process to screen applicants who wish to review the study data. The YODA Project has the final decision-making rights regarding these policies and, by extension, the granting or denial of data requests, as per the contractual agreements between the YODA Project and its partners. Participant-level data sets (appropriately de-identified as per current regional standards to protect patient privacy) will be available. Requestors will be asked to sign a Data Use Agreement (DUA). The DUA explicitly states that access to the data will be used to create or materially enhance generalizable scientific knowledge and that findings derived from analysis will initially be publicly disseminated only through the peer-reviewed biomedical literature or scientific meetings.

It is possible to find more information in the following website:
The YODA Project | Policies & Procedures to Guide External Investigator Access to Clinical Trial Data (yale.edu)

Human research participants

Policy information about studies involving human research participants and Sex and Gender in Research.

Reporting on sex and gender	Only sex- based analysis were performed in the study. There were no discrepacies between gender and sex among participants in this study.
Population characteristics	Participants were mostly men (44 men and 1 female), with a median age of 36 years old, median time with undetectable pVL was 24 months and median CD4 count was 745 cell per µL. All participants were in a INSTI-based ART regimen. Median time from estimated HIV trasmission to ART intiation was 63 days and the percentatge of participants who had at least one beneficial HLA alelle was 22.2%.
Recruitment	All study subjects were recruited from an existing cohort of recently/acute infected individuals who had started antiretroviral treatment within 6 months of acquiring HIV infection (IrsiCaixa/FLS- Early_cART cohort). The study was briefly described by phone or during routine visits at the HIV clinics and if interested, a pre-screening visit was scheduled to all candidates who met the inclusion criteria and none of the exclusion criteria per protocol, avoiding selection biases. During the pre-screening visit the study and procedures were discussed in detail, giving time to think about participation. In a second appointment, the screening visit procedures were performed. Participants were compensated with 50€ or 30€ for each study visit performed on-site or remotely, respectively
Ethics oversight	This study was conducted according to Spanish regulations. Protocol was approved by the local Ethics Committee (Hospital Universitari Germans Trias i Pujol and protocol authorization from Spanish Drug Agency (AEMPs). This study is conforming to the standards of "Good Clinical Practice"by ICH E6. Following the "Good participatory practice guidelines" (published by the Joint United Nations Program on HIV/AIDS (UNAIDS), a Community Advisory Committee (CAC) was called with community stakeholders and representatives from the community HIV/STD screening centers, who participated in the review of the protocol design and informed consents.

Note that full information on the approval of the study protocol must also be provided in the manuscript.

Field-specific reporting

Please select the one below that is the best fit for your research. If you are not sure, read the appropriate sections before making your selection.

☒ Life sciences ☐ Behavioural & social sciences ☐ Ecological, evolutionary & environmental sciences

For a reference copy of the document with all sections, see nature.com/documents/nr-reporting-summary-flat.pdf

Life sciences study design

All studies must disclose on these points even when the disclosure is negative.

Sample size	There was no power calculation for this study. The sample size was proposed to provide preliminary safety information on the vaccine regimen (primary objective. As a means to characterize the statistical properties of this study for the safety primary endpoint, in terms of the chances of observing an AE, 30 participants in the active group provided a high probability (78.5%) that this study would observe at least 1 event if the event occurred in the population with a true rate of 5%. The study size is in line with Guideline on Requirements for First-in-human clinical trials for potential high-risk medicinal products (EMEA/CHMP/SWP/28367/2007). The inclusion of placebo arm ensure that any potential for bias in the analysis of immune responses is minimised and give greater confidence to assignations of the causality of any adverse reactions observed in this study and will help to maintain blinding of the participants.
Data exclusions	1. A woman who is pregnant or breastfeeding at the screening visit. A men or woman who plans to carry out a conception process during the study. 2. When available, pre-cART genotypic data that demonstrates the presence of clinically significant drug resistance mutations that would prevent the construction of a viable cART regimen post-treatment interruption. 3. Reported periods of suboptimal adherence to cART. 4. History of past antiretroviral treatment interruptions longer than 2 weeks.

5. Participation in another clinical trial within 12 weeks of study entry (at screening visit).
6. Any AIDS-defining disease or progression of HIV-related disease.
7. History of autoimmune disease.
8. History or clinical manifestations of any physical or psychiatric disorder which could impair the subject's ability to complete the study.
9. Receipt of approved vaccines within 2 weeks of study entry and along the duration of the trial. (Efforts were made to ensure all participants included are updated on their Hepatitis A, Hepatitis B and Pneumococcal vaccinations before enrolment. Participants willing to undergo seasonal Flu vaccinations or other licensed vaccinations were excluded if vaccination would be expected to occur throughout the duration of the trial. Administration of approved vaccines were allowed during the Roll-over Phase)
10. History of anaphylaxis or severe adverse reaction to vaccines.
11. Previous immunisation with any experimental immunogens.
12. Receipt of blood products within 6 months of study entry.
13. Treatment for cancer or lymphoproliferative disease within 1 year of study entry.
14. Any other current or prior therapy which, in the opinion of the investigators, would make the individual unsuitable for the study or influence the results of the study.
15. Current or recent use (within last 3 months) of interferon or systemic corticosteroids or other immunosuppressive agents (use on inhaled steroids for asthma or topic steroids for localized skin conditions are permitted).
16. Any laboratory abnormalities including:

Haematology
• Haemoglobin < 10.0 g/dl
• Absolute Neutrophil Count (ANC) ≤ 1,000 /mm3 (≤ 1 x 109 /l)
• Absolute Lymphocyte Count (ALC) ≤ 600 /mm3 (≤ 0.6 x 109 /l)
• Platelets ≤100,000 /mm3, ≥ 550,000 /mm3 (≤ 100 /l, ≥ 550 /l)

Biochemistry
• Creatinine > 1.3 x ULN
• Aspartate aminotransferase (AST) > 2.5 x ULN
• Alanine aminotransferase (ALT) > 2.5 x ULN

Microbiology
• Positive for hepatitis B surface antigen,
• Positive for hepatitis C antibody, unless confirmed clearance of HCV infection (spontaneous or following treatment)
• Positive serology indicating active syphilis requiring treatment (Cases in which positive RPR titres were detected but syphilis has been confirmed to have been properly treated were allowed if treatment has been given in the previous two months).

17. (Phase A participants only) Small-pox vaccination.
• Clinical evidence of vaccinia scarification or self-reported history of vaccinia vaccination.

18. (Phase B participants only). Refusal to an eventual cART interruption within the scope of a future study objective. (A questionnaire related to participation in vaccine/cure trials and cART interruptions were performed during the screening visit to be able to address all participant's expectations and worries in a timely manner to reduce the risk of participants lost to follow-up during the trial.)

Prior to enter to Phase C (CCM regimen and ATI) , all of these exclusion criteria were reviewed and the following were added:
1. Virological failure during Phase A/B, defined as 2 consecutive determinations of pVL > 200 cop/ml.
2. Reported periods of suboptimal adherence to cART during Phase A/B.
3. History of antiretroviral treatment interruptions longer than 2 weeks during Phase A/B.
4. Complete refusal to cART interruption..

Replication

ELISPOT and Viral Inhibition immunogenicity assays were run un duplicates or triplicates, as stated in the methods section. Mean value of QC replicates was used for the analysis. ICS flow cytometry was not tested in duplicates for sample availability.

Randomization

Participants were randomized into 2 arms in a 2:1 (vaccine:placebo) ratio.
Subjects were assigned vaccine or placebo through a randomisation schedule based on the randomisation plan using dedicated computer software.
Allocation to active treatment or placebo was maintained throughout the study (Phase A/B/C).

Blinding

Laboratory staff in charge of processing and performing immunogenicity assays, all clinical investigators (including the Principal Investigator – PI-), study nurses administering the IMP, data entry staff and participants were blinded to treatment allocation. Statistics team with randomization tasks had not direct contact with neither participants nor blinded staff. There were designated clinical research associates (CRAs) in charge of monitoring unblinded procedures (randomization, dispensing, IMP preparation and masking).
Only pharmacy staff and unblinding study nurse team (IMP masking and preparation) had unblinding information.

Unblinding of an individual participant was indicated in the event of a medical emergency where the clinical management of the participant would be altered by knowledge of the IMP assignment. The decision to unblind was immediately communicated to the Sponsor and SMC. No emergency unblinding was needed over the study.

Reporting for specific materials, systems and methods

We require information from authors about some types of materials, experimental systems and methods used in many studies. Here, indicate whether each material, system or method listed is relevant to your study. If you are not sure if a list item applies to your research, read the appropriate section before selecting a response.

Materials & experimental systems

n/a	Involved in the study
☐	☒ Antibodies
☒	☐ Eukaryotic cell lines
☒	☐ Palaeontology and archaeology
☒	☐ Animals and other organisms
☐	☒ Clinical data
☒	☐ Dual use research of concern

Methods

n/a	Involved in the study
☒	☐ ChIP-seq
☐	☒ Flow cytometry
☒	☐ MRI-based neuroimaging

Antibodies

Antibodies used

APC-Cy7-labeled anti-human CD3 mAb, Biolegend, Cat#344818, clone SK7, lot# B301842, B285505 and B275133. Dilution 1:333
BV570-labeled anti-human CD4 mAb, Biolegend, Cat# 300534, clone RPA-T4, lot# B319755. Dilution 1:100
BV510-labeled anti-human CD8 mAb, Biolegend, Cat# 301048, clone RPA-T8, lot# B320711, B253532 and B253532. Dilution 1:333
V450-labeled anti-human CD14 mAb, Biolegend, Cat# 325616, clone HCD14, lot# B272019
and B221368. Dilution 1:400
V450-labeled anti-human CD19 mAb, Biolegend, Cat# 302232 , clone HIB19, lot# B275673. Dilution 1:333
BV711-labeled anti-human CCR7 mAb, Biolegend, Cat# 353228, clone GO43H7, lot# B257292
and B303459. Dilution 1:100
BV785-labeled anti-human CD45RA mAb, Biolegend, Cat# 304140, clone HI100, lot# B320193 and B265673. Dilution 1:200
PE-Dazzle-594-labeled anti-human HLADR mAb, Biolegend, Cat# 307654, clone L243, lot# B235176. Dilution 1:250
BV605-labeled anti-human PD1 mAb, Biolegend, Cat# 329924, clone EH12.2H7, lot# B314840. Dilution 1:333
AF700-labeled anti-human IFNg mAb, Invitrogen, Cat# MHCIFG29, clone B27, lot# 2023807 and 2298113. Dilution 1:200
PerCPCy5.5-labeled anti-human IL2 mAb, Biolegend, Cat# 500322, clone MQ1-17H12, lot# B312837. Dilution 1:200
PE -labeled anti-human CD69 mAb, Biolegend, Cat# 310906, clone FN50, lot# B294991. Dilution 1:100
BV650-labeled anti-human CXCR5 (CD185) mAb, BD Biosciences, Cat# 740528, clone RF8B2, lot# 1096639. Dilution 1:2000
PE-Cy7-labeled anti-human TIGIT mAb, ThermoFisher Scientific, Cat# PE-Cy7, clone MBSA43, lot# 2172691. Dilution 1:100
FITC -labeled anti-human Granzyme B mAb, Biolegend, Cat# 515403, clone GB11, lot# B3322790. Dilution 1:35
ALEXA647-labeled anti-human TNF mAb, Biolegend, Cat# 502916, clone MAb11, lot# B301706. Dilution 1:100
Mouse anti-human CD28, BD Bioscience, Cat# 340975, clone L293, lot# 9091671 and 9343750.
Mouse anti-human CD49d, BD BD Bioscience, Cat# 340975, clone L293, lot# 9283590.

Validation

The ICS was performed following SOP multiparametric ICS Flow cytometry for AELIX-002. Manufacturing instructions for each antibody were followed. All antibodies were titrated before use. Whenever the antibody lot was changed, a bridging study was performed.

Validation statements from the manufactures for each antibody:

APC-Cy7-labeled anti-human CD3 mAb, Biolegend, Cat#344818, clone SK7, lot# B301842, B285505 and B275133. Kagoya Y, Nakatsugawa M, Saso K, Guo T, Anczurowski M, Wang CH, Butler MO, Arrowsmith CH, Hirano N. DOT1L inhibition attenuates graft-versus-host disease by allogeneic T cells in adoptive immunotherapy models. Nat Commun. 2018 May 15;9(1):1915.

BV570-labeled anti-human CD4 mAb, Biolegend, Cat# 300534, clone RPA-T4, lot# B319755. Zenaro E, Donini M, Dusi S. Induction of Th1/Th17 immune response by Mycobacterium tuberculosis: role of dectin-1, Mannose Receptor, and DC-SIGN. J Leukoc Biol. 2009 Dec;86(6):1393-401.

BV510-labeled anti-human CD8 mAb, Biolegend, Cat# 301048, clone RPA-T8, lot# B320711, B253532 and B253532. Thakral D, Dobbins J, Devine L, Kavathas PB. Differential expression of the human CD8beta splice variants and regulation of the M-2 isoform by ubiquitination. J Immunol. 2008 Jun 1;180(11):7431-42

V450-labeled anti-human CD14 mAb, Biolegend, Cat# 325616, clone HCD14, lot# B272019
and B221368. John S, Antonia SJ, Rose TA, Seifert RP, Centeno BA, Wagner AS, Creelan BC. Progressive hypoventilation due to mixed CD8+ and CD4+ lymphocytic polymyositis following tremelimumab - durvalumab treatment. J Immunother Cancer. 2017 Jul 18;5(1):54.

V450-labeled anti-human CD19 mAb, Biolegend, Cat# 302232 , clone HIB19, lot# B275673. Joseph A, Zheng JH, Chen K, Dutta M, Chen C, Stiegler G, Kunert R, Follenzi A, Goldstein H. Inhibition of in vivo HIV infection in humanized mice by gene therapy of human hematopoietic stem cells with a lentiviral vector encoding a broadly neutralizing anti-HIV antibody. J Virol. 2010 Jul;84(13):6645-53.

BV711-labeled anti-human CCR7 mAb, Biolegend, Cat# 353228, clone GO43H7, lot# B257292
and B303459. de Mingo Pulido Á, Gardner A, Hiebler S, Soliman H, Rugo HS, Krummel MF, Coussens LM, Ruffell B. TIM-3 Regulates CD103+ Dendritic Cell Function and Response to Chemotherapy in Breast Cancer. Cancer Cell. 2018 Jan 8;33(1):60-74.e6.

BV785-labeled anti-human CD45RA mAb, Biolegend, Cat# 304140, clone HI100, lot# B320193 and B265673. Roque S, Nobrega C, Appelberg R, Correia-Neves M. IL-10 underlies distinct susceptibility of BALB/c and C57BL/6 mice to Mycobacterium avium infection

and influences efficacy of antibiotic therapy. J Immunol. 2007 Jun 15;178(12):8028-35.

PE-Dazzle-594-labeled anti-human HLADR mAb, Biolegend, Cat# 307654, clone L243, lot# B235176. Zaba LC, Cardinale I, Gilleaudeau P, Sullivan-Whalen M, Suárez-Fariñas M, Fuentes-Duculan J, Novitskaya I, Khatcherian A, Bluth MJ, Lowes MA, Krueger JG. Amelioration of epidermal hyperplasia by TNF inhibition is associated with reduced Th17 responses. J Exp Med. 2007 Dec 24;204(13):3183-94

BV605-labeled anti-human PD1 mAb, Biolegend, Cat# 329924, clone EH12.2H7, lot# B314840. Zahn RC, Rett MD, Korioth-Schmitz B, Sun Y, Buzby AP, Goldstein S, Brown CR, Byrum RA, Freeman GJ, Letvin NL, Hirsch VM, Schmitz JE. Simian immunodeficiency virus (SIV)-specific CD8+ T-cell responses in vervet African green monkeys chronically infected with SIVagm. J Virol. 2008 Dec;82(23):11577-88.

AF700-labeled anti-human IFNg mAb, Invitrogen, Cat# MHCIFG29, clone B27, lot# 2023807 and 2298113. He X, Li D, Luo Z, Liang H, Peng H, Zhao Y, Wang N, Liu D, Qin C, Wei Q, Yan H, Shao Y. Compromised NK cell-mediated antibody-dependent cellular cytotoxicity in chronic SIV/SHIV infection. PLoS One. 2013;8(2):e56309.

PerCPCy5.5-labeled anti-human IL2 mAb, Biolegend, Cat# 500322, clone MQ1-17H12, lot# B312837. Dzhagalov I, Chambon P, He YW. Regulation of CD8+ T lymphocyte effector function and macrophage inflammatory cytokine production by retinoic acid receptor gamma. J Immunol. 2007 Feb 15;178(4):2113-21.

PE -labeled anti-human CD69 mAb, Biolegend, Cat# 310906, clone FN50, lot# B294991. Lu H, Crawford RB, North CM, Kaplan BL, Kaminski NE. Establishment of an immunoglobulin m antibody-forming cell response model for characterizing immunotoxicity in primary human B cells. Toxicol Sci. 2009 Dec;112(2):363-73.

BV650-labeled anti-human CXCR5 (CD185) mAb, BD Biosciences, Cat# 740528, clone RF8B2, lot# 1096639. Barella L, Loetscher M, Tobler A, Baggiolini M, Moser B. Sequence variation of a novel heptahelical leucocyte receptor through alternative transcript formation. Biochem J. 1995 Aug 1;309 (Pt 3)(Pt 3):773-9.

PE-Cy7-labeled anti-human TIGIT mAb, ThermoFisher Scientific, Cat# PE-Cy7, clone MBSA43, lot# 2172691. Tauriainen J, Scharf L, Frederiksen J, Naji A, Ljunggren HG, Sönnerborg A, Lund O, Reyes-Terán G, Hecht FM, Deeks SG, Betts MR, Buggert M, Karlsson AC. Perturbed CD8+ T cell TIGIT/CD226/PVR axis despite early initiation of antiretroviral treatment in HIV infected individuals. Sci Rep. 2017 Jan 13;7:40354.

FITC -labeled anti-human Granzyme B mAb, Biolegend, Cat# 515403, clone GB11, lot# B3322790. Wiede F, Ziegler A, Zehn D, Tiganis T. PTPN2 restrains CD8$^+$ T cell responses after antigen cross-presentation for the maintenance of peripheral tolerance in mice. J Autoimmun. 2014 Sep;53:105-14.

ALEXA647-labeled anti-human TNF mAb, Biolegend, Cat# 502916, clone MAb11, lot# B301706. Iwamoto S, Iwai S, Tsujiyama K, Kurahashi C, Takeshita K, Naoe M, Masunaga A, Ogawa Y, Oguchi K, Miyazaki A. TNF-alpha drives human CD14+ monocytes to differentiate into CD70+ dendritic cells evoking Th1 and Th17 responses. J Immunol. 2007 Aug 1;179(3):1449-57.

Clinical data

Policy information about clinical studies

All manuscripts should comply with the ICMJE guidelines for publication of clinical research and a completed CONSORT checklist must be included with all submissions.

Clinical trial registration	NCT03204617
Study protocol	Version 7.0, 3rd February 2020 (last version) - submitted as S1. List of study amendments also provided as S2
Data collection	The study was conducted at Hospital Universitari Germans Trias i Pujol, Badalona, Barcelona. The community center Barcelona Checkpoint was a supporting center during ATI visits. Protocol approval/authorization: 05/06/2017 Contract signed: 28/06/2017 Clinical SIV: 30/06/2017 First vaccination: 28/08/2017 Interim report (week 32): 28/06/2018 First participant ATI started: 23/09/2019 Last subject last visit: 10/03/2021
Outcomes	This was an exploratory study with the primary endpoint is to evaluate the safety and tolerability of HIV-1 vaccine DNA.HTI administered IM alone and as part of a heterologous prime-boost regimen with MVA.HTI and ChAdOx1.HTI in early treated HIV-1 positive individuals (DDDMM and CCM). Safety was assessed by an analysis of local and systemic reactogenicity and laboratory data. Participants are monitored for AEs and SAEs during the study. All solicited local and systemic AEs are recorded from the time of administration of each IMP and within 7 days thereafter in a "Participant reactogenicity diary card". AEs assessment (severity/ causality) is based according the Division of DAIDS table for grading the severity of adult and pediatric adverse events, Version 2.1. [March 2017]. Secondary study endpoint included immunogenicity of DDDMM+CCM and effect on viral rebound during an ATI

-Immunogenicity of DDDMM+CCM was assessed by the proportion of participants that developed de-novo T cell responses to HTI-encoded regions measured by IFNg ELISPOT assay. Breadth and magnitude of total vaccine induced HIV-specific responses measured by IFNg ELISPOT too.

-The effect on viral rebound during ATI was evaluated by the following endpoints:
- Percentage of participants with viral remission, defined as plasma viral load (pVL) <50 copies/mL 12 and 24 weeks after start of ATI.
- Percentage of participants with viral control, defined as a pVL <2,000 copies/mL at 12 and 24 weeks after ATI.
- Time to viral detection, defined as the time from ATI start to first occurrence of detectable pVL (>50 copies/mL).
- Time to viral rebound, defined as the time from ATI start to first occurrence of pVL > 10,000 copies/mL.
- Percentage of participants who remain off cART at 12 and 24 weeks after ATI (efficacy endpoint).
- Time off cART, defined as time to cART resumption since ATI start (efficacy endopoint).

Flow Cytometry

Plots

Confirm that:

☒ The axis labels state the marker and fluorochrome used (e.g. CD4-FITC).

☒ The axis scales are clearly visible. Include numbers along axes only for bottom left plot of group (a 'group' is an analysis of identical markers).

☒ All plots are contour plots with outliers or pseudocolor plots.

☒ A numerical value for number of cells or percentage (with statistics) is provided.

Methodology

Sample preparation	Cryopreserved PBMCs from week 28 (4 weeks after completion of last series of vaccinations, DDDMM-CCM) were used for the stimulation with 4 pools spanning different HIV-1 proteins/sub-proteins of 9-43 peptides per pool corresponding to p17, p24/p15, Pol and Vif/Nef regions included in the HTI vaccine insert. Peptides were added at a final concentration of 5ug/ml of each peptide in the presence of both, 1.4µg/ml of anti-CD28 (BD Bioscience) and 1.4µg/ml anti-CD49d (BD Bioscience). As positive controls for the assay, cells were cultured alone in the presence of 1) anti-CD3/28 Dynabeads (Thermo Fisher Scientific) according to manufacturer´s instructions or 2) 10ng/ml PMA (SIGMA) and 1µM Ionomycin (SIGMA). Cells stimulated with only anti-CD28 and anti-CD49d antibodies or with DMSO were used as the negative controls. Stimulated cells were incubated for 6 h at 37℃ in 5% CO2, in the presence of 4µl of monensin (GolgiStop, BD Bioscience). After 6 hours of stimulation, cells were incubated with Live/Dead fixable Violet Dead cell stain kit (Invitrogen), for exclusion of dead cells, along with the exclusion of monocytes and B cells by including in the dump channel anti-CD14 and anti-CD19 antibodies. Surface markers of T cell linage (CD3, CD4 and CD8), follicular T cells (CXCR5 and PD1), T cell phenotype (CD45RA and CCR7), T cell activation (CD69 and HLADR) and T cell exhaustion (TIGIT, PD1) were included as well. Cells were fix and permeabilized using the Cell Fixation and Cell Permeabilization Kit (Invitrogen) and intracellularly stained for INF-γ, GrazymeB, IL-2 and TNF-α. Cells were resuspended in PBS supplemented with 1%FBS
Instrument	Cells were acquired on a LSR Fortessa flow cytometer (BD)
Software	The frequencies of cells that produce all possible combinations of intracellular cytokines were calculated using Boolean gating function of the FlowJo software. Preprocessing of flow cytometry data was performed using both FlowJo software version 10.6 and imported into Pestle2/ SPICE software v5.35 (Vaccine Research Center, NIAID/NIH, Bethesda, MD, USA) for graphical representation
Cell population abundance	At least 100,000 total events were recorde
Gating strategy	When needed for variably expressed antigens, fluorescence minus one (FMO) was included to define boundaries between positive and negative populations. A forward scatter height (FSC-H) vs forward scatter area (FSC-A) plot was used to exclude doublets. Then an FSC-A vs side scatter area (SSC-A) plot was used to select PBMCs. Live CD3+ cells were gated with the dump channel, which allowed exclusion of dead cells, monocytes (CD14), and B cells (CD19). Within the live CD3+ cell population, expression of CD4 and CD8 was then determined. The evaluation of cytokine production (INF-γ, GzmB, IL-2, and TNFα) (b) in CD4+ and CD8+ T cell populations from unstimulated and anti-CD3/CD28 stimulated conditions in one representative participant is shown in Extended data Fig 7

☒ Tick this box to confirm that a figure exemplifying the gating strategy is provided in the Supplementary Information.